13

SPREAD SPECTRUM SIGNALS FOR DIGITAL COMMUNICATIONS

Spread spectrum signals used for the transmission of digital information are distinguished by the characteristic that their bandwidth W is much greater than the information rate R in bits/s. That is, the bandwidth expansion factor $B_e = W/R$ for a spread spectrum signal is much greater than unity. The large redundancy inherent in spread spectrum signals is required to overcome the severe levels of interference that are encountered in the transmission of digital information over some radio and satellite channels. Since coded waveforms are also characterized by a bandwidth expansion factor greater than unity and since coding is an efficient method for introducing redundancy, it follows that coding is an important element in the design of spread spectrum signals.

A second important element employed in the design of spread spectrum signals is pseudo-randomness, which makes the signals appear similar to random noise and difficult to demodulate by receivers other than the intended ones. This element is intimately related with the application or purpose of such signals.

To be specific, spread spectrum signals are used for

- combatting or suppressing the detrimental effects of interference due to jamming, interference arising from other users of the channel, and self-interference due to multipath propagation;
- hiding a signal by transmitting it at low power and, thus, making it difficult for an unintended listener to detect in the presence of background noise;
- achieving message privacy in the presence of other listeners.

In applications other than communications, spread spectrum signals are used

to obtain accurate range (time delay) and range rate (velocity) measurements in radar and navigation. For the sake of brevity, we shall limit our discussion to digital communications applications.

In combatting intentional interference (jamming), it is important to the communicators that the jammer who is trying to disrupt the communication does not have prior knowledge of the signal characteristics except for the overall channel bandwidth and the type of modulation, (PSK, FSK, etc.) being used. If the digital information is just encoded as described in Chapter 8, a sophisticated jammer can easily mimic the signal emitted by the transmitter and, thus, confuse the receiver. To circumvent this possibility, the transmitter introduces an element of unpredictability or randomness (pseudo-randomness) in each of the transmitted coded signal waveforms that is known to the intended receiver but not to the jammer. As a consequence, the jammer must synthesize and transmit an interfering signal without knowledge of the pseudo-random pattern.

Interference from the other users arises in multiple-access communication systems in which a number of users share a common channel bandwidth. At any given time, a subset of these users may transmit information simultaneously over the common channel to corresponding receivers. Assuming that all the users employ the same code for the encoding and decoding of their respective information sequences, the transmitted signals in this common spectrum may be distinguished from one another by superimposing a different pseudo-random pattern, also called a *code*, in each transmitted signal. Thus, a particular receiver can recover the transmitted information intended for it by knowing the pseudo-random pattern, i.e., the key, used by the corresponding transmitter. This type of communication technique, which allows multiple users to simultaneously use a common channel for transmission of information, is called *code division multiple access* (CDMA). CDMA will be considered in Sections 13-2 and 13-3.

Resolvable multipath components resulting from time-dispersive propagation through a channel may be viewed as a form of self-interference. This type of interference may also be suppressed by the introduction of a pseudo-random pattern in the transmitted signal, as will be described below.

A message may be hidden in the background noise by spreading its bandwidth with coding and transmitting the resultant signal at a low average power. Because of its low power level, the transmitted signal is said to be "covert." It has a low probability of being intercepted (detected) by a casual listener and, hence, is also called a *low-probability-of-intercept* (LPI) signal.

Finally, message privacy may be obtained by superimposing a pseudo-random pattern on a transmitted message. The message can be demodulated by the intended receivers, who know the pseudo-random pattern or key used at the transmitter, but not by any other receivers who do not have knowledge of the key.

In the following sections, we shall describe a number of different types of spread spectrum signals, their characteristics, and their application. The

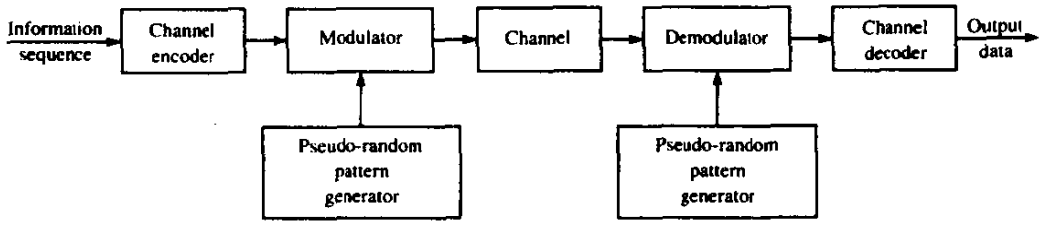

FIGURE 13-1-1 Model of spread spectrum digital communication system.

emphasis will be on the use of spread spectrum signals for combatting, jamming (antijam or AJ signals), for CDMA, and for LPI. Before discussing the signal design problem, however, we shall briefly describe the types of channel characteristics assumed for the applications cited above.

13-1 MODEL OF SPREAD SPECTRUM DIGITAL COMMUNICATION SYSTEM

The block diagram shown in Fig. 13-1-1 illustrates the basic elements of a spread spectrum digital communication system with a binary information sequence at its input at the transmitting end and at its output at the receiving end. The channel encoder and decoder and the modulator and demodulator are basic elements of the system, which were treated in Chapters 5, 7 and 8. In addition to these elements, we have two identical pseudo-random pattern generators, one that interfaces with the modulator at the transmitting end and a second that interfaces with the demodulator at the receiving end. The generators generate a pseudo-random or pseudo-noise (PN) binary-valued sequence, which is impressed on the transmitted signal at the modulator and removed from the received signal at the demodulator.

Synchronization of the PN sequence generated at the receiver with the PN sequence contained in the incoming received signal is required in order to demodulate the received signal. Initially, prior to the transmission of information, synchronization may be achieved by transmitting a fixed pseudo-random bit pattern that the receiver will recognize in the presence of interference with a high probability. After time synchronization of the generators is established, the transmission of information may commence.

Interference is introduced in the transmission of the information-bearing signal through the channel. The characteristics of the interference depend to a large extent on its origin. It may be categorized as being either broadband or narrowband relative to the bandwidth of the information-bearing signal, and either continuous or pulsed (discontinuous) in time. For example, a jamming signal may consist of one or more sinusoids in the bandwidth used to transmit the information. The frequencies of the sinusoids may remain fixed or they may change with time according to some rule. As a second example, the interference generated in CDMA by other users of the channel may be either

broadband or narrowband, depending on the type of spread spectrum signal that is employed to achieve multiple access. If it is broadband, it may be characterized as an equivalent additive white gaussian noise. We shall consider these types of interference and some others in the following sections.

Our treatment of spread spectrum signals will focus on the performance of the digital communication system in the presence of narrowband and broadband interference. Two types of modulation are considered: PSK and FSK. PSK is appropriate in applications where phase coherence between the transmitted signal and the received signal can be maintained over a time interval that is relatively long compared to the reciprocal of the transmitted signal bandwidth. On the other hand, FSK modulation is appropriate in applications where such phase coherence cannot be maintained due to time-variant effects on the communications link. This may be the case in a communications link between two high-speed aircraft or between a high-speed aircraft and a ground terminal.

The PN sequence generated at the modulator is used in conjunction with the PSK modulation to shift the phase of the PSK signal pseudo-randomly as described in Section 13-2. The resulting modulated signal is called a *direct sequence* (DS) or a *pseudo-noise* (PN) spread spectrum signal. When used in conjunction with binary or M-ary ($M > 2$) FSK, the pseudo-random sequence selects the frequency of the transmitted signal pseudo-randomly. The resulting signal is called a *frequency-hopped* (FH) spread spectrum signal. Although a number of other types of spread spectrum signals will be briefly described, the emphasis of our treatment will be on PN and FH spread spectrum signals.

13-2 DIRECT SEQUENCE SPREAD SPECTRUM SIGNALS

In the model shown in Fig. 13-1-1, we assume that the information rate at the input to the encoder is R bits/s and the available channel bandwidth is W Hz. The modulation is assumed to be binary PSK. In order to utilize the entire available channel bandwidth, the phase of the carrier is shifted pseudo-randomly according to the pattern from the PN generator at a rate W times/s. The reciprocal of W, denoted by T_c, defines the duration of a rectangular pulse, which is called a *chip* while T_c is called the *chip interval*. The pulse is the basic element in a DS spread spectrum signal.

If we define $T_b = 1/R$ to be the duration of a rectangular pulse corresponding to the transmission time of an information bit, the bandwidth expansion factor W/R may be expressed as

$$B_e = \frac{W}{R} = \frac{T_b}{T_c} \tag{13-2-1}$$

In practical systems, the ratio T_b/T_c is an integer,

$$L_c = \frac{T_b}{T_c} \tag{13-2-2}$$

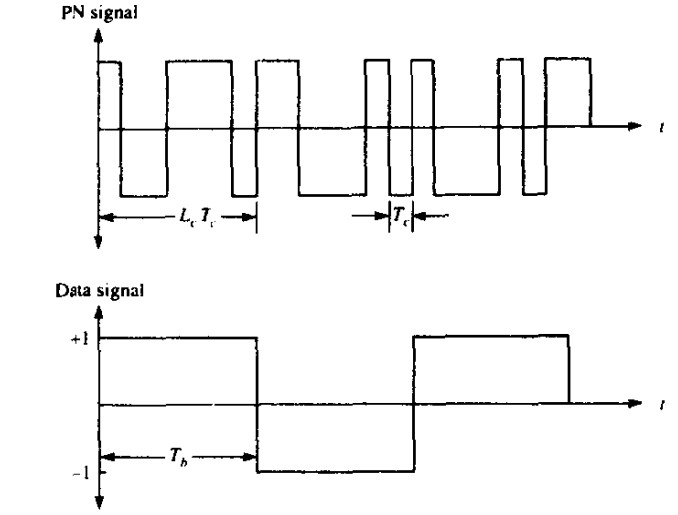

(a) PN and data signals

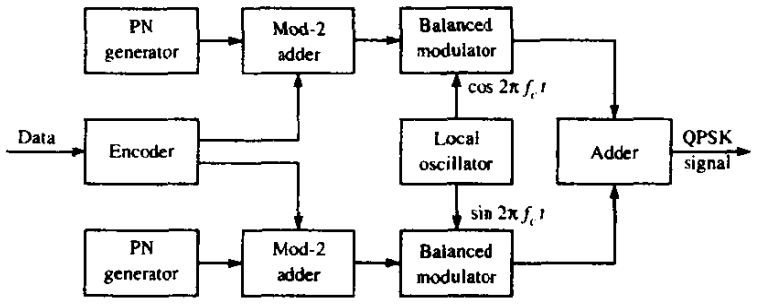

(b) DS-QPSK modulator

FIGURE 13-2-1 The PN and data signals (*a*) and the QPSK modulator (*b*) for a DS spread spectrum system.

which is the number of chips per information bit. That is, L_c is the number of phase shifts that occur in the transmitted signal during the bit duration $T_b = 1/R$. Figure 13-2-1(*a*) illustrates the relationships between the PN signal and the data signal.

Suppose that the encoder takes k information bits at a time and generates a binary linear (n, k) block code. The time duration available for transmitting the n code elements is kT_b s. The number of chips that occur in this time interval is kL_c. Hence, we may select the block length of the code as $n = kL_c$. If the encoder generates a binary convolutional code of rate k/n, the number of chips in the time interval kT_b is also $n = kL_c$. Therefore, the following discussion applies to both block codes and convolutional codes.

One method for impressing the PN sequence on the transmitted signal is to

alter directly the coded bits by modulo-2 addition with the PN sequence.† Thus, each coded bit is altered by its addition with a bit from the PN sequence. If b_i represents the ith bit of the PN sequence and c_i is the corresponding bit from the encoder, the modulo-2 sum is

$$a_i = b_i \oplus c_i \tag{13-2-3}$$

Hence, $a_i = 1$ if either $b_i = 1$ and $c_i = 0$ or $b_i = 0$ and $c_i = 1$; also, $a_i = 0$ if either $b_i = 1$ and $c_i = 1$ or $b_i = 0$ and $c_i = 0$. We may say that $a_i = 0$ when $b_i = c_i$ and $a_i = 1$ when $b_i \neq c_i$. The sequence $\{a_i\}$ is mapped into a binary PSK signal of the form $s(t) = \pm \text{Re}\,[g(t)e^{j2\pi f_c t}]$ according to the convention

$$g_i(t) = \begin{cases} g(t - iT_c) & (a_i = 0) \\ -g(t - iT_c) & (a_i = 1) \end{cases} \tag{13-2-4}$$

where $g(t)$ represents a pulse of duration T_c s and arbitrary shape.

The modulo-2 addition of the coded sequence $\{c_i\}$ and the sequence $\{b_i\}$ from the PN generator may also be represented as a multiplication of two waveforms. To demonstrate this point, suppose that the elements of the coded sequence are mapped into a binary PSK signal according to the relation

$$c_i(t) = (2c_i - 1)g(t - iT_c) \tag{13-2-5}$$

Similarly, we define a waveform $p_i(t)$ as

$$p_i(t) = (2b_i - 1)p(t - iT_c) \tag{13-2-6}$$

where $p(t)$ is a rectangular pulse of duration T_c. Then the equivalent lowpass transmitted signal corresponding to the ith coded bit is

$$\begin{aligned} g_i(t) &= p_i(t)c_i(t) \\ &= (2b_i - 1)(2c_i - 1)g(t - iT_c) \end{aligned} \tag{13-2-7}$$

This signal is identical to the one given by (13-2-4), which is obtained from the sequence $\{a_i\}$. Consequently, modulo-2 addition of the coded bits with the PN sequence followed by a mapping that yields a binary PSK signal is equivalent to multiplying a binary PSK signal generated from the coded bits with a sequence of unit amplitude rectangular pulses, each of duration T_c, and with a polarity which is determined from the PN sequence according to (13-2-6). Although it is easier to implement modulo-2 addition followed by PSK modulation instead of waveform multiplication, it is convenient, for purposes of demodulation, to consider the transmitted signal in the multiplicative form

† When four-phase PSK is desired, one PN sequence is added to the information sequence carried on the in-phase signal component and a second PN sequence is added to the information sequence carried on the quadrature component. In many PN-spread spectrum systems, the same binary information sequence is added to the two PN sequences to form the two quadrature components. Thus, a four-phase PSK signal is generated with a binary information stream.

given by (13-2-7). A functional block diagram of a four-phase PSK DS spread spectrum modulator is shown in Fig. 13-2-1(*b*).

The received equivalent lowpass signal for the ith code element is†

$$\begin{aligned} r_i(t) &= p_i(t)c_i(t) + z(t), \qquad iT_c \leq t \leq (i+1)T_c \\ &= (2b_i - 1)(2c_i - 1)g(t - iT_c) + z(t) \end{aligned} \tag{13-2-8}$$

where $z(t)$ represents the interference or jamming signal corrupting the information-bearing signal. The interference is assumed to be a stationary random process with zero mean.

If $z(t)$ is a sample function from a complex-valued gaussian process, the optimum demodulator may be implemented either as a filter matched to the waveform $g(t)$ or as a correlator, as illustrated by the block diagrams in Fig. 13-2-2. In the matched filter realization, the sampled output from the matched filter is multiplied by $2b_i - 1$, which is obtained from the PN generator at the

FIGURE 13-2-2 Possible demodulator structures for PN spread spectrum signals.

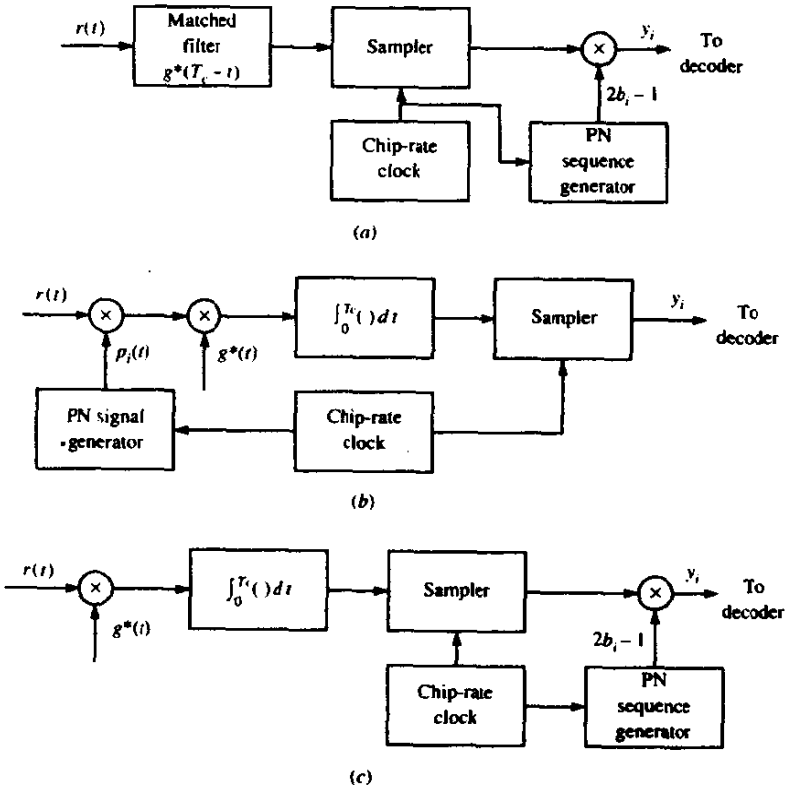

† *For simplicity, we assume that the channel attenuation* $\alpha = 1$ *and the phase shift of the channel is zero. Since coherent PSK detection is assumed, any arbitrary channel phase shift is compensated for in the demodulation.*

demodulator when the PN generator is properly synchronized. Since $(2b_i - 1)^2 = 1$ when $b_i = 0$ and $b_i = 1$, the effect of the PN sequence on the received coded bits is thus removed.

In Fig. 13-2-2, we also observe that the cross-correlation can be accomplished in either one of two ways. The first, illustrated in Fig. 13-2-2(b), involves premultiplying $r_i(t)$ with the waveform $p_i(t)$ generated from the output of the PN generator and then cross-correlating with $g^*(t)$ and sampling the output in each chip interval. The second method, illustrated in Fig. 13-2-2(c), involves cross-correlation with $g^*(t)$ first, sampling the output of the correlator and, then, multiplying this output with $2b_i - 1$, which is obtained from the PN generator.

If $z(t)$ is not a gaussian random process, the demodulation methods illustrated in Fig. 13-2-2 are no longer optimum. Nevertheless, we may still use any of these three demodulator structures to demodulate the received signal. When the statistical characteristics of the interference $z(t)$ are unknown a priori, this is certainly one possible approach. An alternative method, which is described later, utilizes an adaptive filter prior to the matched filter or correlator to suppress narrowband interference. The rationale for this second method is also described later.

In Section 13-2-1, we derive the error rate performance of the DS spread spectrum system in the presence of wideband and narrowband interference. The derivations are based on the assumption that the demodulator is any of the three equivalent structures shown in Fig. 13-2-2.

13-2-1 Error Rate Performance of the Decoder

Let the unquantized output of the demodulator be denoted by y_j, $1 \leq j \leq n$. First we consider a linear binary (n, k) block code and, without loss of generality, we assume that the all-zero code word is transmitted.

A decoder that employs soft-decision decoding computes the correlation metrics

$$CM_i = \sum_{j=1}^{n} (2c_{ij} - 1)y_j, \qquad i = 1, 2, \ldots, 2^k \tag{13-2-9}$$

where c_{ij} denotes the jth bit in the ith code word. The correlation metric corresponding to the all-zero code word is

$$\begin{aligned} CM_1 &= 2n\mathscr{E}_c + \sum_{j=1}^{n} (2c_{1j} - 1)(2b_j - 1)v_j \\ &= 2n\mathscr{E}_c - \sum_{j=1}^{n} (2b_j - 1)v_j \end{aligned} \tag{13-2-10}$$

where v_j, $1 \leq j \leq n$, is the additive noise term corrupting the jth coded bit and $\mathscr{E}_c$ is the chip energy. It is defined as

$$v_j = \text{Re}\left\{\int_0^{T_c} g^*(t)z[t + (j-1)T_c]\,dt\right\}, \qquad j = 1, 2, \ldots, n \tag{13-2-11}$$

Similarly, the correlation metric corresponding to code word $\mathbf{C}_m$ having weight w_m is

$$CM_m = 2\mathscr{E}_c n\left(1 - \frac{2w_m}{n}\right) + \sum_{j=1}^{n} (2c_{mj} - 1)(2b_j - 1)v_j \qquad (13\text{-}2\text{-}12)$$

Following the procedure used in Section 8-1-4, we shall determine the probability that $CM_m > CM_1$. The difference between CM_1 and CM_m is

$$\begin{aligned} D &= CM_1 - CM_m \\ &= 4\mathscr{E}_c w_m - 2\sum_{j=1}^{n} c_{mj}(2b_j - 1)v_j \end{aligned} \qquad (13\text{-}2\text{-}13)$$

Since the code word $\mathbf{C}_m$ has weight w_m, there are w_m nonzero components in the summation of noise terms contained in (13-2-13). We shall assume that the minimum distance of the code is sufficiently large that we can invoke the central limit theorem for the summation of noise components. This assumption is valid for PN spread spectrum signals that have a bandwidth expansion of 20 or more.† Thus, the summation of noise components is modeled as a gaussian random variable. Since $E(2b_j - 1) = 0$ and $E(v_j) = 0$, the mean of the second term in (13-2-13) is also zero.

The variance is

$$\sigma_m^2 = 4\sum_{j=1}^{n}\sum_{i=1}^{n} c_{mi}c_{mj}E[(2b_j - 1)(2b_i - 1)]E(v_i v_j) \qquad (13\text{-}2\text{-}14)$$

The sequence of binary digits from the PN generator are assumed to be uncorrelated. Hence,

$$E[(2b_j - 1)(2b_i - 1)] = \delta_{ij} \qquad (13\text{-}2\text{-}15)$$

and

$$\sigma_m^2 = 4w_m E(v^2) \qquad (13\text{-}2\text{-}16)$$

where $E(v^2)$ is the second moment of any one element from the set $\{v_j\}$. This moment is easily evaluated to yield

$$\begin{aligned} E(v^2) &= \int_0^{T_c}\int_0^{T_c} g^*(t)g(\tau)\phi_{zz}(t - \tau)\,dt\,d\tau \\ &= \int_{-\infty}^{\infty} |G(f)|^2\,\Phi_{zz}(f)\,df \end{aligned} \qquad (13\text{-}2\text{-}17)$$

† Typically, the bandwidth expansion factor in a spread spectrum signal is of the order of 100 and higher.

where $\phi_{zz}(\tau) = \frac{1}{2}E[z^*(t)z(t+\tau)]$ is the autocorrelation function and $\Phi_{zz}(f)$ is the power spectral density of the interference $z(t)$.

We observe that when the interference is spectrally flat within the bandwidth† occupied by the transmitted signal, i.e.,

$$\Phi_{zz}(f) = J_0 \qquad |f| \leq \tfrac{1}{2}W \tag{13-2-18}$$

the second moment in (13-2-17) is $E(v^2) = 2\mathscr{E}_c J_0$, and, hence, the variance of the interference term in (13-2-16) becomes

$$\sigma_m^2 = 8\mathscr{E}_c J_0 w_m \tag{13-2-19}$$

In this case, the probability that $D < 0$ is

$$P_2(m) = Q\left(\sqrt{\frac{2\mathscr{E}_c}{J_0} w_m}\right) \tag{13-2-20}$$

But the energy per coded bit $\mathscr{E}_c$ may be expressed in terms of the energy per information bit $\mathscr{E}_b$ as

$$\mathscr{E}_c = \frac{k}{n}\mathscr{E}_b = R_c\mathscr{E}_b \tag{13-2-21}$$

With this substitution, (13-2-20) becomes

$$\begin{aligned} P_2(m) &= Q\left(\sqrt{\frac{2\mathscr{E}_b}{J_0} R_c w_m}\right) \\ &= Q(\sqrt{2\gamma_b R_c w_m}) \end{aligned} \tag{13-2-22}$$

where $\gamma_b = \mathscr{E}_b/J_0$ is the SNR per information bit. Finally, the code word error probability may be upper-bounded by the union bound as

$$P_m \leq \sum_{m=2}^{M} Q(\sqrt{2\gamma_b R_c w_m}) \tag{13-2-23}$$

where $M = 2^k$. Note that this expression is identical to the probability of a code word error for soft-decision decoding of a linear binary block code in an AWGN channel.

Although we have considered a binary block code in the derivation given above, the procedure is similar for an (n, k) convolutional code. The result of such a derivation is the following upper bound on the equivalent bit error probability:

$$P_b \leq \frac{1}{k}\sum_{d=d_{\text{free}}}^{\infty} \beta_d Q(\sqrt{2\gamma_b R_c d}) \tag{13-2-24}$$

The set of coefficients $\{\beta_d\}$ is obtained from an expansion of the derivative of the transfer function $T(D, N)$, as described in Section 8-2-3.

Next, we consider a narrowband interference centered at the carrier (at d.c.

† If the bandwidth of the bandpass channel is W, that of the equivalent low-pass channel is $\frac{1}{2}W$.

for the equivalent lowpass signal). We may fix the total (average) jamming power to $J_{av} = J_0 W$, where J_0 is the value of the power spectral density of an equivalent wideband interference (jamming signal). The narrowband interference is characterized by the power spectral density

$$\Phi_{zz}(f) = \begin{cases} \dfrac{J_{av}}{W_1} = \dfrac{J_0 W}{W_1} & (|f| \leq \frac{1}{2}W_1) \\ 0 & (|f| > \frac{1}{2}W_1) \end{cases} \tag{13-2-25}$$

where $W \gg W_1$.

Substitution of (13-2-25) for $\Phi_{zz}(f)$ into (13-2-17) yields

$$E(v^2) = \frac{J_{av}}{W_1} \int_{-W_1/2}^{W_1/2} |G(f)|^2 \, df \tag{13-2-26}$$

The value of $E(v^2)$ depends on the spectral characteristics of the pulse $g(t)$. In the following example, we consider two special cases.

Example 13-2-1

Suppose that $g(t)$ is a rectangular pulse as shown in Fig. 13-2-3(a) and $|G(f)|^2$ is the corresponding energy density spectrum shown in Fig. 13-2-3(b). For the narrowband interference given by (13-2-26), the variance of the total interference is

$$\begin{aligned} \sigma_m^2 &= 4w_m E(v^2) \\ &= \frac{8\mathscr{E}_c w_m T_c J_{av}}{W_1} \int_{-W_1/2}^{W_1/2} \left(\frac{\sin \pi f T_c}{\pi f T_c}\right)^2 df \\ &= \frac{8\mathscr{E}_c w_m J_{av}}{W_1} \int_{-\beta/2}^{\beta/2} \left(\frac{\sin \pi x}{\pi x}\right)^2 dx \end{aligned} \tag{13-2-27}$$

FIGURE 13-2-3 Rectangular pulse and its energy density spectrum.

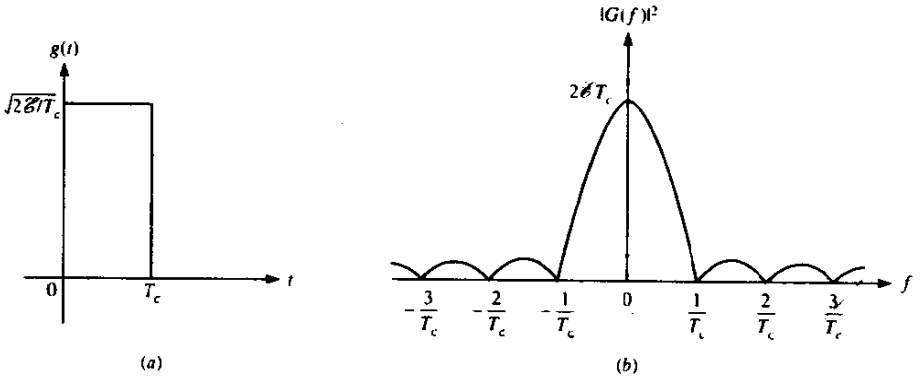

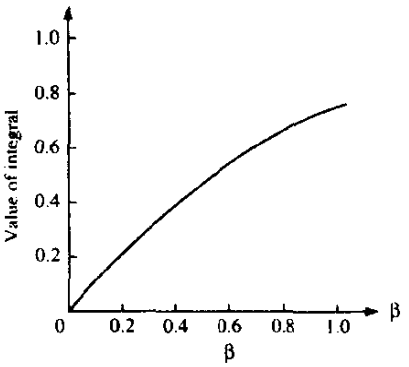

FIGURE 13-2-4 Plot of the value of the integral in (13-2-27).

where $\beta = W_1 T_c$. Figure 13-2-4 illustrates the value of this integral for $0 \leq \beta \leq 1$. We observe that the value of the integral is upper-bounded by $W_1 T_c$. Hence, $\sigma_m^2 \leq 8\mathscr{E}_c w_m T_c J_{av}$.

In the limit as W_1 becomes zero, the interference becomes an impulse at the carrier. In this case the interference is a pure frequency tone and it is usually called a *CW jamming signal.* The power spectral density is

$$\Phi_{zz}(f) = J_{av}\delta(f) \tag{13-2-28}$$

and the corresponding variance for the decision variable $D = CM_1 - CM_m$ is

$$\begin{aligned}\sigma_m^2 &= 4w_m J_{av} |G(0)|^2 \\ &= 8w_m \mathscr{E}_c T_c J_{av}\end{aligned} \tag{13-2-29}$$

The probability of a code word error for CW jamming is upper-bounded as

$$P_M \leq \sum_{m=2}^{M} Q\left(\sqrt{\frac{2\mathscr{E}_c}{J_{av}T_c}\, w_m}\right) \tag{13-2-30}$$

But $\mathscr{E}_c = R_c \mathscr{E}_b$. Furthermore, $T_c \approx 1/W$ and $J_{av}/W = J_0$. Therefore (13-2-30) may be expressed as

$$P_M \leq \sum_{m=2}^{M} Q\left(\sqrt{\frac{2\mathscr{E}_b}{J_0} R_c w_m}\right) \tag{13-2-31}$$

which is the result obtained previously for broadband interference. This result indicates that a CW jammer has the same effect on performance as an equivalent broadband jammer. This equivalence is discussed further below.

Example 13-2-2

Let us determine the performance of the DS spread spectrum system in the presence of a CW jammer of average power J_{av} when the transmitted signal pulse $g(t)$ is one-half cycle of a sinusoid as illustrated in Fig. 13-2-5, i.e.,

$$g(t) = \sqrt{\frac{4\mathscr{E}_c}{T_c}} \sin\frac{\pi t}{T_c}, \qquad 0 \leq t \leq T_c \tag{13-2-32}$$

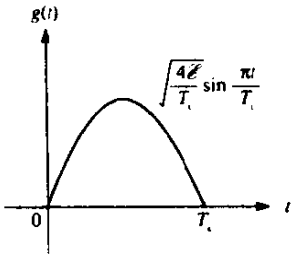

FIGURE 13-2-5 A sinusoidal signal pulse.

The variance of the interference of this pulse is

$$\sigma_m^2 = 4w_m J_{av} |G(0)|^2$$
$$= \frac{64}{\pi^2} \mathscr{E}_c T_c J_{av} w_m \tag{13-2-33}$$

Hence, the upper bound on the code word error probability is

$$P_M \leq \sum_{m=2}^{M} Q\left(\sqrt{\frac{\pi^2 \mathscr{E}_b}{4J_{av}T_c} R_c w_m}\right) \tag{13-2-34}$$

We observe that the performance obtained with this pulse is 0.9 dB better than that obtained with a rectangular pulse. Recall that this pulse shape when used in offset QPSK results in an MSK signal. MSK modulation is frequently used in DS spread spectrum systems.

The Processing Gain and the Jamming Margin An interesting interpretation of the performance characteristics for the DS spread spectrum signal is obtained by expressing the signal energy per bit $\mathscr{E}_b$ in terms of the average power. That is, $\mathscr{E}_b = P_{av}T_b$, where P_{av} is the average signal power and T_b is the bit interval. Let us consider the performance obtained in the presence of CW jamming for the rectangular pulse treated in Example 13-2-1. When we substitute for $\mathscr{E}_b$ and J_0 into (13-2-31), we obtain

$$P_M \leq \sum_{m=2}^{M} Q\left(\sqrt{\frac{2P_{av}}{J_{av}}\frac{T_b}{T_c} R_c w_m}\right) = \sum_{m=2}^{M} Q\left(\sqrt{\frac{2P_{av}}{J_{av}} L_c R_c w_m}\right) \tag{13-2-35}$$

where L_c is the number of chips per information bit and P_{av}/J_{av} is the signal-to-jamming power ratio.

An identical result is obtained with broadband jamming for which the performance is given by (13-2-23). For the signal energy per bit, we have

$$\mathscr{E}_b = P_{av}T_b = \frac{P_{av}}{R} \tag{13-2-36}$$

where R is the information rate in bits/s. The power spectral density for the jamming signal may be expressed as

$$J_0 = \frac{J_{av}}{W} \tag{13-2-37}$$

Using the relation in (13-2-36) and (13-2-37), the ratio $\mathscr{E}_b/J_0$ may be expressed as

$$\frac{\mathscr{E}_b}{J_0} = \frac{P_{av}/R}{J_{av}/W} = \frac{W/R}{J_{av}/P_{av}} \tag{13-2-38}$$

The ratio J_{av}/P_{av} is the jamming-to-signal power ratio, which is usually greater than unity. The ratio $W/R = T_b/T_c = B_c = L_c$ is just the bandwidth expansion factor, or, equivalently, the number of chips per information bit. This ratio is usually called the *processing gain* of the DS spread spectrum system. It represents the advantage gained over the jammer that is obtained by expanding the bandwidth of the transmitted signal. If we interpret $\mathscr{E}_b/J_0$ as the SNR required to achieve a specified error rate performance and W/R as the available bandwidth expansion factor, the ratio J_{av}/P_{av} is called the *jamming margin* of the DS spread spectrum system. In other words, the jamming margin is the largest value that the ratio J_{av}/P_{av} can take and still satisfy the specified error probability.

The performance of a soft-decision decoder for a linear (n, k) binary code, expressed in terms of the processing gain and the jamming margin, is

$$P_m \leq \sum_{m=2}^{M} Q\left(\sqrt{\frac{2W/R}{J_{av}/P_{av}} R_c w_m}\right) \leq (M-1)Q\left(\sqrt{\frac{2W/R}{J_{av}/P_{av}} R_c d_{min}}\right) \tag{13-2-39}$$

In addition to the processing gain W/R and J_{av}/P_{av}, we observe that the performance depends on a third factor, namely, $R_c w_m$. This factor is the *coding gain*. A lower bound on this factor is $R_c d_{min}$. Thus the jamming margin achieved by the DS spread spectrum signal depends on the processing gain and the coding gain.

Uncoded DS Spread Spectrum Signals The performance results given above for DS spread spectrum signals generated by means of an (n, k) code may be specialized to a trivial type of code, namely, a binary repetition code. For this case, $k = 1$ and the weight of the nonzero code word is $w = n$. Thus, $R_c w = 1$ and, hence, the performance of the binary signaling system reduces to

$$\begin{aligned} P_2 &= Q\left(\sqrt{\frac{2\mathscr{E}_b}{J_0}}\right) \\ &= Q\left(\sqrt{\frac{2W/R}{J_{av}/P_{av}}}\right) \end{aligned} \tag{13-2-40}$$

Note that the trivial (repetition) code gives no coding gain. It does result in a processing gain of W/R.

Example 13-2-3

Suppose that we wish to achieve an error rate performance of 10^{-6} or less with an uncoded DS spread spectrum system. The available bandwidth expansion factor is $W/R = 1000$. Let us determine the jamming margin.

The $\mathscr{E}_b/J_0$ required to achieve a bit error probability of 10^{-6} with uncoded binary PSK is 10.5 dB. The processing gain is $10 \log_{10} 1000 = 30$ dB. Hence the maximum jamming-to-signal power that can be tolerated, i.e., the jamming margin, is

$$10 \log_{10} \frac{J_{av}}{P_{av}} = 30 - 10.5 = 19.5 \text{ dB}$$

Since this is the jamming margin achieved with an uncoded DS spread spectrum system, it may be increased by coding the information sequence.

There is another way to view the modulation and demodulation processes for the uncoded (repetition code) DS spread spectrum system. At the modulator, the signal waveform generated by the repetition code with rectangular pulses, for example, is identical to a unit amplitude rectangular pulse $s(t)$ of duration T_b or its negative, depending on whether the information bit is 1 or 0, respectively. This may be seen from (13-2-7), where the coded chips $\{c_i\}$ within a single information bit are either all 1s or 0s. The PN sequence multiplies either $s(t)$ or $-s(t)$. Thus, when the information bit is a 1, the L_c PN chips generated by the PN generator are transmitted with the same polarity. On the other hand, when the information bit is a 0, the L_c PN chips when multiplied by $-s(t)$ are reversed in polarity.

The demodulator for the repetition code, implemented as a correlator, is illustrated in Fig. 13-2-6. We observe that the integration interval in the integrator is the bit interval T_b. Thus, the decoder for the repetition code is eliminated and its function is subsumed in the demodulator.

Now let us qualitatively assess the effect of this demodulation process on

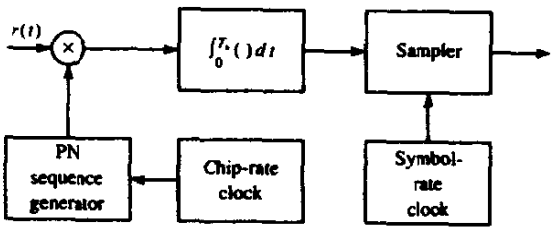

FIGURE 13-2-6 Correlation-type demodulator for a repetition code.

the interference $z(t)$. The multiplication of $z(t)$ by the output of the PN generator, which is expressed as

$$w(t) = \sum_i (2b_i - 1)p(t - iT_c)$$

yields

$$v(t) = w(t)z(t)$$

The waveforms $w(t)$ and $z(t)$ are statistically independent random processes each with zero mean and autocorrelation functions $\phi_{ww}(\tau)$ and $\phi_{zz}(\tau)$, respectively. The product $v(t)$ is also a random process having an autocorrelation function equal to the product of $\phi_{ww}(\tau)$ with $\phi_{zz}(\tau)$. Hence, the power spectral density of the process $v(t)$ is equal to the convolution of the power spectral density of $w(t)$ with the power spectral density of $z(t)$.

The effect of convolving the two spectra is to spread the power in bandwidth. Since the bandwidth of $w(t)$ occupies the available channel bandwith W, the result of convolution of the two spectra is to spread the power spectral density of $z(t)$ over the frequency band of width W. If $z(t)$ is a narrowband process, i.e., its power spectral density has a width much less than W, the power spectral density of the process $v(t)$ will occupy a bandwidth equal to at least W.

The integrator used in the cross-correlation shown in Fig. 13-2-6 has a bandwidth approximately equal to $1/T_b$. Since $1/T_b \ll W$, only a fraction of the total interference power appears at the output of the correlator. This fraction is approximately equal to the ratio of bandwidths $1/T_b$ to W. That is,

$$\frac{1/T_b}{W} = \frac{1}{WT_b} = \frac{T_c}{T_b} = \frac{1}{L_c}$$

In other words, the multiplication of the interference with the signal from the PN generator spreads the interference to the signal bandwidth W, and the narrowband integration following the multiplication sees only the fraction $1/L_c$ of the total interference. Thus, the performance of the uncoded DS spread spectrum system is enhanced by the processing gain L_c.

Linear Code Concatenated with a Binary Repetition Code As illustrated above, a binary repetition code provides a margin against an interference or jamming signal but yields no coding gain. To obtain an improvement in performance, we may use a linear (n_1, k) block or convolutional code, where $n_1 \leq n = kL_c$. One possibility is to select $n_1 < n$ and to repeat each code bit n_2 times such that $n = n_1 n_2$. Thus, we can construct a linear (n_1, k) code by concatenating the (n_1, k) code with a binary $(n_2, 1)$ repetition code. This may be viewed as a trivial form of code concatenation where the outer code is the (n_1, k) code and the inner code is the repetition code.

Since the repetition code yields no coding gain, the coding gain achieved by the combined code must reduce to that achieved by the (n_1, k) outer code. It

is demonstrated that this is indeed the case. The coding gain of the overall combined code is

$$R_c w_m = \frac{k}{n} w_m, \qquad m = 2, 3, \ldots, 2^k$$

But the weights $\{w_m\}$ for the combined code may be expressed as

$$w_m = n_2 w_m^0$$

where $\{w_m^0\}$ are the weights of the outer code. Therefore, the coding gain of the combined code is

$$R_c w_m = \frac{k}{n_1 n_2} n_2 w_m^0 = \frac{k}{n_1} w_m^0 = R_c^0 w_m^0 \tag{13-2-41}$$

which is just the coding gain obtained from the outer code.

A coding gain is also achieved if the (n_1, k) outer code is decoded using hard decisions. The probability of a bit error obtained with the $(n_2, 1)$ repetition code (based on soft-decision decoding) is

$$\begin{aligned} p &= Q\left(\sqrt{\frac{2n_2 \mathscr{E}_c}{J_0}}\right) = Q\sqrt{\frac{2\mathscr{E}_b}{J_0} R_c^0}\Big) \\ &= Q\left(\sqrt{\frac{2W/R}{J_{av}/P_{av}} R_c^0}\right) \end{aligned} \tag{13-2-42}$$

Then the code word error probability for a linear (n_1, k) block code is upper-bounded as

$$P_M \leq \sum_{m=t+1}^{n_1} \binom{n_1}{m} p^m (1-p)^{n_1 - m} \tag{13-2-43}$$

where $t = \lfloor \frac{1}{2}(d_{\min} - 1) \rfloor$, or as

$$P_M \leq \sum_{m=2}^{M} [4p(1-p)]^{w_m^0/2} \tag{13-2-44}$$

where the latter is a Chernoff bound. For an (n_1, k) binary convolutional code, the upper bound on the bit error probability is

$$P_b \leq \sum_{d=d_{\text{free}}}^{\infty} \beta_d P_2(d) \tag{13-2-45}$$

where $P_2(d)$ is defined by (8-2-28) for odd d and by (8-2-29) for even d.

Concatenated Coding for DS Spread Spectrum Systems It is apparent from the above discussion that an improvement in performance can be obtained by replacing the repetition code by a more powerful code that will

yield a coding gain in addition to the processing gain. Basically, the objective in a DS spread spectrum system is to construct a long, low-rate code having a large minimum distance. This may be best accomplished by using code concatenation. When binary PSK is used in conjunction with DS spread spectrum, the elements of a concatenated code word must be expressed in binary form.

Best performance is obtained when soft-decision decoding is used on both the inner and outer codes. However, an alternative, which usually results in reduced complexity for the decoder, is to employ soft-decision decoding on the inner code and hard-decision decoding on the outer code. The expressions for the error rate performance of these decoding schemes depend, in part, on the type of codes (block or convolutional) selected for the inner and outer codes. For example, the concatenation of two block codes may be viewed as an overall long binary (n, k) block code having a performance given by (13-2-39). The performance of other code combinations may also be readily derived. For the sake of brevity, we shall not consider such code combinations.

13-2-2 Some Applications of DS Spread Spectrum Signals

In this subsection, we shall briefly consider the use of coded DS spread spectrum signals for three specific applications. One is concerned with providing immunity against a jamming signal. In the second, a communication signal is hidden in the background noise by transmitting the signal at a very low power level. The third application is concerned with accommodating a number of simultaneous signal transmissions on the same channel, i.e., CDMA.

Antijamming Application In Section 13-2-1, we derived the error rate performance for a DS spread spectrum signal in the presence of either a narrow band or a wideband jamming signal. As examples to illustrate the performance of a digital communications system in the presence of a jamming signal, we shall select three codes. One is the Golay (24, 12), which is characterized by the weight distribution given in Table 8-1-1 and has a minimum distance $d_{\min} = 8$. The second code is an expurgated Golay (24, 11) obtained by selecting 2048 code words of constant weight 12. Of course this expurgated code is nonlinear. These two codes will be used in conjunction with a repetition code. The third code to be considered is a maximum-length shift-register code.

The error rate performance of the Golay (24, 12) with soft-decision decoding is

$$P_M \leq \left[759Q\left(\sqrt{\frac{8W/R}{J_{av}/P_{av}}}\right) + 2576Q\left(\sqrt{\frac{12W/R}{J_{av}/P_{av}}}\right) + 759Q\left(\sqrt{\frac{16W/R}{J_{av}/P_{av}}}\right) + Q\left(\sqrt{\frac{24W/R}{J_{av}/P_{av}}}\right)\right] \tag{13-2-46}$$

where W/R is the processing gain and J_{av}/P_{av} is the jamming margin. Since $n = n_1 n_2 = 12W/R$ and $n_1 = 24$, each coded bit is, in effect, repeated $n_2 = W/2R$ times. For example, if $W/R = 100$ (a processing gain of 20 dB), the block length of the repetition code is $n_2 = 50$.

If hard-decision decoding is used, the probability of error for a coded bit is

$$p = Q\left(\sqrt{\frac{W/R}{J_{av}/P_{av}}}\right) \tag{13-2-47}$$

and the corresponding probability of a code word error is upper-bounded as

$$P_M \leq \sum_{m=4}^{24} \binom{24}{m} p^m (1-p)^{24-m} \tag{13-2-48}$$

As an alternative, we may use the Chernoff bound for hard-decision decoding, which is

$$\begin{aligned} P_M \leq\ & 759[4p(1-p)]^4 + 2576[4p(1-p)]^6 \\ & + 759[4p(1-p)]^8 + [4p(1-p)]^{12} \end{aligned} \tag{13-2-49}$$

Figure 13-2-7 illustrates the performance of the Golay (24, 12) as a function of the jamming margin J_{av}/P_{av}, with the processing gain as a parameter. The Chernoff bound was used to compute the error probability for hard-decision decoding. The error probability for soft-decision decoding is dominated by the term

$$759Q\left(\sqrt{\frac{8W/R}{J_{av}/P_{av}}}\right)$$

and that for hard-decision decoding is dominated by the term $759[4p(1-p)]^4$. Hence, the coding gain for soft-decision decoding † is at most $10 \log 4 = 6$ dB. We note that the two curves corresponding to $W/R = 1000$ (30 dB) are identical in shape to the ones for $W/R = 100$ (20 dB), except that the latter are shifted by 10 dB to the right relative to the former. This shift is simply the difference in processing gain between these two DS spread spectrum signals.

The error rate performance of the expurgated Golay (24, 11) is upper-bounded as

$$P_M \leq 2047Q\left(\sqrt{\frac{11W/R}{J_{av}/P_{av}}}\right) \tag{13-2-50}$$

for soft-decision decoding and as‡

$$P_M \leq 2047[4p(1-p)]^6 \tag{13-2-51}$$

† The coding gain is less than 6 dB due to the multiplicative factor of 759, which increases the error probability relative to the performance of the binary uncoded system.

‡ We remind the reader that the union bound is not very tight for large signal sets.

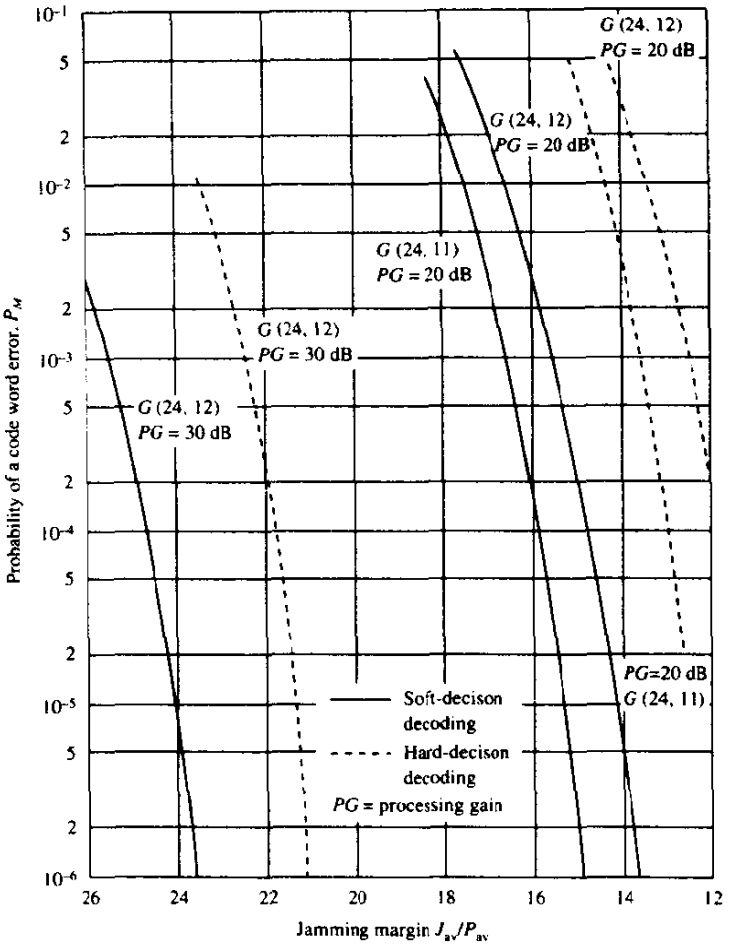

FIGURE 13-2-7 Performance of Golay codes used in DS spread spectrum signal.

for hard-decision decoding, where p is given as

$$p = Q\left(\sqrt{\frac{11W/R}{J_{av}/P_{av}}}\right) \tag{13-2-52}$$

The performance characteristics of this code are also plotted in Fig. 13-2-7 for $W/R = 100$. We observe that this expurgated Golay (24, 11) code performs about 1 dB better than the Golay (24, 12) code.

Instead of using a block code concatenated with a low-rate $(1/n_2)$ repetition code, let us consider using a single low-rate code. A particularly suitable set of low-rate codes is the set of maximum-length shift-register codes described in Section 8-1-3. We recall that for this set of codes,

$$\begin{aligned}(n, k) &= (2^m - 1, m)\\ d_{\min} &= 2^{m-1}\end{aligned} \tag{13-2-53}$$

All code words except the all-zero word have an identical weight of 2^{m-1}. Hence, the error rate for soft-decision decoding is upper-bounded as†

$$P_M \leq (M-1)Q\left(\sqrt{\frac{2W/R}{J_{av}/P_{av}} R_c d_{min}}\right)$$

$$\leq 2^m Q\left(\sqrt{\frac{2W/R}{J_{av}/P_{av}} \frac{m2^{m-1}}{2^m-1}}\right)$$

$$\leq 2^m \exp\left(-\frac{W/R}{J_{av}/P_{av}} \frac{m2^{m-1}}{2^m-1}\right) \qquad (13\text{-}2\text{-}54)$$

For moderate values of m, $R_c d_{min} \approx \frac{1}{2}m$ and, hence, (13-2-54) may be expressed as

$$P_M \leq 2^m Q\left(\sqrt{\frac{W/R}{J_{av}/P_{av}} m}\right) \leq 2^m \exp\left(-\frac{mW/R}{2J_{av}P_{av}}\right) \qquad (13\text{-}2\text{-}55)$$

Hence, the coding gain is at most $10 \log \frac{1}{2}m$.

For example, if we select $m = 10$ then $n = 2^{10} - 1 = 1023$. Since $n = kW/R = mW/R$, it follows that $W/R \approx 102$. Thus, we have a processing gain of about 20 dB and a coding gain of 7 dB. This performance is comparable to that obtained with the expurgated Golay (24, 11) code. Higher coding gains can be achieved with larger values of m.

If hard-decision decoding is used for the maximum-length shift-register codes, the error rate is upper-bounded by the Chernoff bound as

$$P_M \leq (M-1)[4p(1-p)]^{d_{min}/2} = (2^m - 1)[4p(1-p)]^{2^{m-2}} \qquad (13\text{-}2\text{-}56)$$

where p is given as

$$p = Q\left(\sqrt{\frac{2W/R}{J_{av}/P_{av}} R_c}\right) = Q\left(\sqrt{\frac{2W/R}{J_{av}/P_{av}} \frac{m}{2^m-1}}\right) \qquad (13\text{-}2\text{-}57)$$

For $m = 10$, the code word error rate P_M is comparable to that obtained with the expurgated Golay (24, 11) code for hard-decision decoding.

The reslts given above illustrate the performance that can be obtained with a single level of coding. Greater coding gains can be achieved with concatenated codes.

† The $M = 2^m$ waveforms generated by a maximum-length shift-register code form a simplex set (see Problem 8-13). The exact expression for the error probability, given in Section 5-2-4, may be used for large values of M, where the union bound becomes very loose.

Low-Detectability Signal Transmission In this application, the signal is purposely transmitted at a very low power level relative to the background channel noise and thermal noise that is generated in the front end of the receiver. If the DS spread spectrum signal occupies a bandwidth W and the spectral density of the additive noise is N_0 W/Hz, the average noise power in the bandwidth W is $N_{av} = WN_0$.

The average received signal power at the intended receiver is P_{av}. If we wish to hide the presence of the signal from receivers that are in the vicinity of the intended receiver, the signal is transmitted at a low power level such that $P_{av}/N_{av} \ll 1$. The intended receiver can recover the information-bearing signal with the aid of the processing gain and the coding gain. However, any other receiver that has no prior knowledge of the PN sequence is unable to take advantage of the processing gain and the coding gain. Hence, the presence of the information-bearing signal is difficult to detect. We say that the signal has a *low probability* of being *intercepted* (LPI) and it is called an *LPI signal.*

The probability of error results given in Section 13-2-1 also apply to the demodulation and decoding of LPI signals at the intended receiver.

Code Division Multiple Access The enhancement in performance obtained from a DS spread spectrum signal through the processing gain and coding gain can be used to enable many DS spread spectrum signals to occupy the same channel bandwidth provided that each signal has its own distinct PN sequence. Thus, it is possible to have several users transmit messages simultaneously over the same channel bandwidth. This type of digital communication in which each user (transmitter-receiver pair) has a distinct PN code for transmitting over a common channel bandwidth is called either *code division multiple access* (CDMA) or *spread spectrum multiple access* (SSMA).

In the demodulation of each PN signal, the signals from the other simultaneous users of the channel appear as an additive interference. The level of interference varies, depending on the number of users at any given time. A major advantage of CDMA is that a large number of users can be accommodated if each transmits messages for a short period of time. In such a multiple access system, it is relatively easy either to add new users or to decrease the number of users without disrupting the system.

Let us determine the number of simultaneous signals that can be supported in a CDMA system.† For simplicity, we assume that all signals have identical average powers. Thus, if there are N_u simultaneous users, the desired signal-to-noise interference power ratio at a given receiver is

$$\frac{P_{av}}{J_{av}} = \frac{P_{av}}{(N_u - 1)P_{av}} = \frac{1}{N_u - 1} \tag{13-2-58}$$

† In this section the interference from other users is treated as a random process. This is the case if there is no cooperation among the users. In Chapter 15 we consider CDMA transmission in which interference from other users is known and is suppressed by the receiver.

Hence, the performance for soft-decision decoding at the given receiver is upper-bounded as

$$P_M \leq \sum_{m=2}^{M} Q\left(\sqrt{\frac{2W/R}{N_u - 1} R_c w_m}\right) \leq (M-1) Q\left(\sqrt{\frac{2W/R}{N_u - 1} R_c d_{\min}}\right) \tag{13-2-59}$$

In this case, we have assumed that the interference from other users is gaussian.

As an example, suppose that the desired level of performance (error probability of 10^{-6}) is achieved when

$$\frac{W/R}{N_u - 1} R_c d_{\min} = 20$$

Then the maximum number of users that can be supported in the CDMA system is

$$N_u = \frac{W/R}{20} R_c d_{\min} + 1 \tag{13-2-60}$$

If $W/R = 100$ and $R_c d_{\min} = 4$, as obtained with the Golay (24, 12) code, the maximum number is $N_u = 21$. If $W/R = 1000$ and $R_c d_{\min} = 4$, this number becomes $N_u = 201$.

In determining the maximum number of simultaneous users of the channel, we have implicitly assumed that the PN code sequences are mutually orthogonal and the interference from other users adds on a power basis only. However, orthogonality among a number of PN code sequences is not easily achieved, especially if the number of PN code sequences required is large. In fact, the selection of a good set of PN sequences for a CDMA system is an important problem that has received considerable attention in the technical literature. We shall briefly discuss this problem in Section 13-2-3.

13-2-3 Effect of Pulsed Interference on DS Spread Spectrum Systems

Thus far, we have considered the effect of continuous interference or jamming on a DS spread spectrum signal. We have observed that the processing gain and coding gain provide a means for overcoming the detrimental effects of this type of interference. However, there is a jamming threat that has a dramatic effect on the performance of a DS spread spectrum system. That jamming signal consists of pulses of spectrally flat noise that covers the entire signal bandwidth W. This is usually called *pulsed interference* or *partial-time jamming*.

Suppose the jammer has an average power J_{av} in the signal bandwidth W. Hence $J_0 = J_{av}/W$. Instead of transmitting continuously, the jammer transmits pulses at a power J_{av}/α for $\alpha\%$ of the time, i.e., the probability that the jammer is transmitting at a given instant is α. For simplicity, we assume that

an interference pulse spans an integral number of signaling intervals and, thus, it affects an integral number of bits. When the jammer is not transmitting, the transmitted bits are assumed to be received error-free, and when the jammer is transmitting, the probability of error for an uncoded DS spread spectrum system is $Q(\sqrt{2\alpha\mathscr{E}_b/J_0})$. Hence, the average probability of a bit error is

$$P_2(\alpha) = \alpha Q(\sqrt{2\alpha\mathscr{E}_b/J_0}) = \alpha Q\left(\sqrt{\frac{2\alpha W/R}{J_{av}/P_{av}}}\right) \tag{13-2-61}$$

The jammer selects the duty cycle α to maximize the error probability. On differentiating (13-2-61) with respect to α, we find that the worst-case pulse jamming occurs when

$$\alpha^* = \begin{cases} \dfrac{0.71}{\mathscr{E}_b/J_0} & (\mathscr{E}_b/J_0 \geq 0.71) \\ 1 & (\mathscr{E}_b/J_0 < 0.71) \end{cases} \tag{13-2-62}$$

and the corresponding error probability is

$$P_2 = \begin{cases} \dfrac{0.083}{\mathscr{E}_b/J_0} = \dfrac{0.083 J_{av}/P_{av}}{W/R} & (\mathscr{E}_b/J_0 > 0.71) \\ Q\left(\sqrt{\dfrac{2W/R}{J_{av}/P_{av}}}\right) & (\mathscr{E}_b/J_0 < 0.71) \end{cases} \tag{13-2-63}$$

The error rate performance given by (13-2-61) for $\alpha = 1.0$, 0.1, and 0.01 along with the worst-case performance based on α^* is plotted in Fig. 13-2-8.

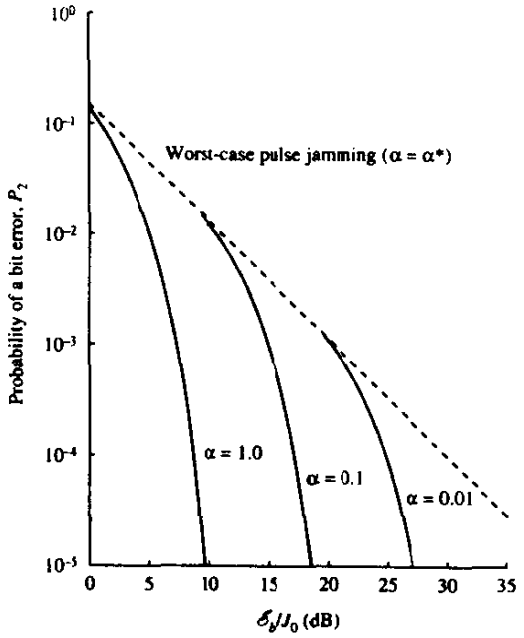

FIGURE 13-2-8 Performance of DS binary PSK with pulse jamming.

By comparing the error rate for continuous gaussian noise jamming with worst-case pulse jamming, we observe a large difference in performance, which is approximately 40 dB at an error rate of 10^{-6}.

We should point out that the above analysis applies when the jammer pulse duration is equal to or greater than the bit duration. In addition, we should indicate that practical considerations may prohibit the jammer from achieving high peak power (small values of α). Nevertheless, the error probability given by (13-2-63) serves as an upper bound on the performance of the uncoded binary PSK in worst-case pulse jamming. Clearly, the performance of the DS spread spectrum system in the presence of such jamming is extremely poor.

If we simply add coding to the DS spread spectrum system, the improvement over the uncoded system is the coding gain. Thus, $\mathscr{E}_b/J_0$ is reduced by the coding gain, which in most cases is limited to less than 10 dB. The reason for the poor performance is that the jamming signal pulse duration may be selected to affect many consecutive coded bits when the jamming signal is turned on. Consequently, the code word error probability is high due to the burst characteristics of the jammer.

In order to improve the performance, we should interleave the coded bits prior to transmission over the channel. The effect of the interleaving, as discussed in Section 8-1-9, is to make the coded bits that are hit by the jammer statistically independent.

The block diagram of the digital communication system that includes interleaving/deinterleaving is shown in Fig. 13-2-9. Also shown is the possibility that the receiver knows the jammer state, i.e., that it knows when the jammer is on or off. Knowledge of the jammer state (called *side information*) is sometimes available from channel measurements of noise power levels in adjacent frequency bands. In our treatment, we consider two

FIGURE 13-2-9 Block diagram of AJ communication system.

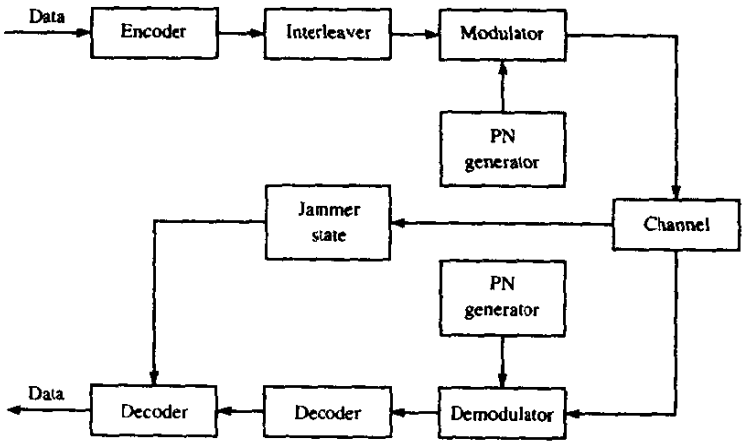

extreme cases, namely, no knowledge of the jammer state or complete knowledge of the jammer state. In any case, the random variable ζ representing the jammer state is characterized by the probabilities

$$P(\zeta = 1) = \alpha, \quad P(\zeta = 0) = 1 - \alpha$$

When the jammer is on, the channel is modeled as an AWGN with power spectral density $N_0 = J_0/\alpha = J_{av}/\alpha W$; and when the jammer is off, there is no noise in the channel. Knowledge of the jammer state implies that the decoder knows when $\zeta = 1$ and when $\zeta = 0$, and uses this information in the computation of the correlation metrics. For example, the decoder may weight the demodulator output for each coded bit by the reciprocal of the noise power level in the interval. Alternatively, the decoder may give zero weight (erasure) to a jammed bit.

First, let us consider the effect of jamming without knowledge of the jammer state. The interleaver/deinterleaver pair is assumed to result in statistically independent jammer hits of the coded bits. As an example of the performance achieved with coding, we cite the performance results from the paper of Martin and McAdam (1980). There the performance of binary convolutional codes is evaluated for worst-case pulse jamming. Both hard and soft-decision Viterbi decoding are considered. Soft decisions are obtained by quantizing the demodulator output to eight levels. For this purpose, a uniform quantizer is used for which the threshold spacing is optimized for the pulse jammer noise level. The quantizer plays the important role of limiting the size of the demodulator output when the pulse jammer is on. The limiting action ensures that any hit on a coded bit does not heavily bias the corresponding path metrics.

The optimum duty cycle for the pulse jammer in the coded system is generally inversely proportional to the SNR, but its value is different from that given by (13-2-62) for the uncoded system. Figure 13-2-10 illustrates graphically the optimal jammer duty cycle for both hard- and soft-decision decoding of the rate 1/2 convolutional codes. The corresponding error rate results for this worst-case pulse jammer are illustrated in Figs 13-2-11 and 13-2-12 for rate 1/2 codes with constraint lengths $3 \leq K \leq 9$. For example, note that at $P_2 = 10^{-6}$, the $K = 7$ convolutional code with soft-decision decoding requires $\mathscr{E}_b/J_0 = 7.6$ dB, whereas hard-decision decoding requires $\mathscr{E}_b/J_0 = 11.7$ dB. This 4.1 dB difference in SNR is relatively large. With continuous gaussian noise, the corresponding SNRs for an error rate of 10^{-6} are 5 dB for soft-decision decoding and 7 dB for hard-decision decoding. Hence, the worst-case pulse jammer has degraded the performance by 2.6 dB for soft-decision decoding and by 4.7 dB for hard-decision decoding. These levels of degradation increase as the constraint length of the convolutional code is decreased. The important point, however, is that the loss in SNR due to jamming has been reduced from 40 dB for the uncoded system to less than 5 dB for the coded system based on a $K = 7$, rate 1/2 convolutional code.

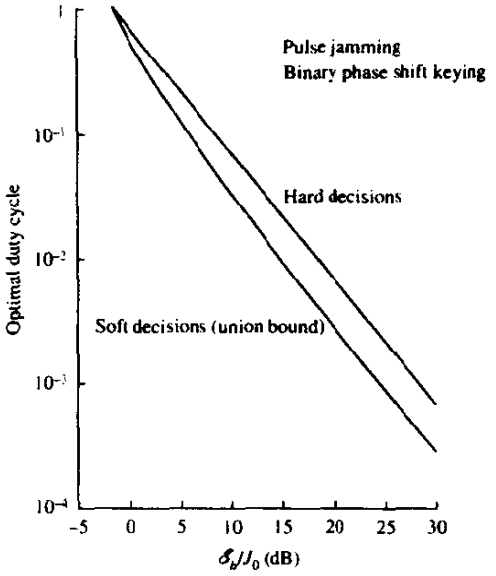

FIGURE 13-2-10 Optimal duty cycle for pulse jammer. [*From Martin and McAdam (1980). © 1980 IEEE.*]

A simpler method for evaluating the performance of a coded AJ communication system is to use the cutoff rate parameter R_0 as proposed by Omura and Levitt (1982). For example, with binary-coded modulation, the cutoff rate may be expressed as

$$R_0 = 1 - \log(1 + D_\alpha) \tag{13-2-64}$$

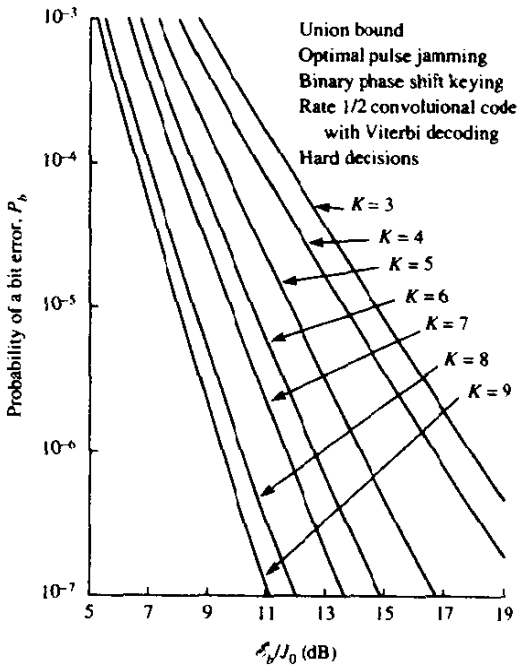

FIGURE 13-2-11 Performance of rate 1/2 convolutional codes with hard-decision Viterbi decoding binary PSK with optimal pulse jamming. [*From Martin and McAdam (1980). © 1980 IEEE.*]

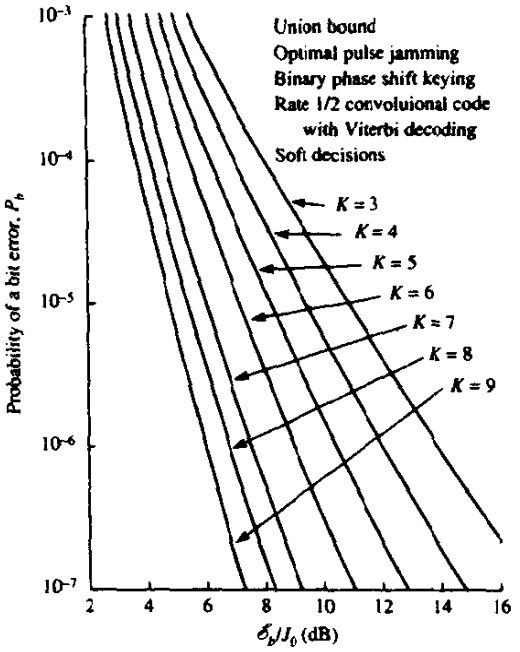

FIGURE 13-2-12 Performance of rate 1/2 convolutional codes with soft-decision Viterbi decoding binary PSK with optimal pulse jamming. [*From Martin and McAdam (1980). © 1980 IEEE.*]

where the factor D_α depends on the channel noise characteristics and the decoder processing. Recall that for binary PSK in an AWGN channel and soft-decision decoding,

$$D_\alpha = e^{-\mathscr{E}_c/N_0} \tag{13-2-65}$$

where $\mathscr{E}_c$ is the energy per coded bit; and for hard-decision decoding,

$$D_\alpha = \sqrt{4p(1-p)} \tag{13-2-66}$$

where p is the probability of a coded bit error. Here, we have $N_0 \equiv J_0$.

For a coded binary PSK, with pulse jamming, Omura and Levitt (1982) have shown that

$$D_\alpha = \alpha e^{-\alpha \mathscr{E}_c/N_0} \quad \text{for soft-decision decoding with knowledge of jammer state} \tag{13-2-67}$$

$$D_\alpha = \min_{\lambda \geq 0} \{[\alpha \exp(\lambda^2 \mathscr{E}_c N_0/\alpha) + 1 - \alpha] \exp(-2\lambda \mathscr{E}_c)\}$$

for soft-decision decoding with no knowledge of jammer state (13-2-68)

$$D_\alpha = \alpha\sqrt{4p(1-p)} \quad \text{for hard-decision decoding with knowledge of the jammer state} \tag{13-2-69}$$

$$D_\alpha = \sqrt{4\alpha p(1-\alpha p)} \quad \text{for hard-decision decoding with no knowledge of the jammer state} \tag{13-2-70}$$

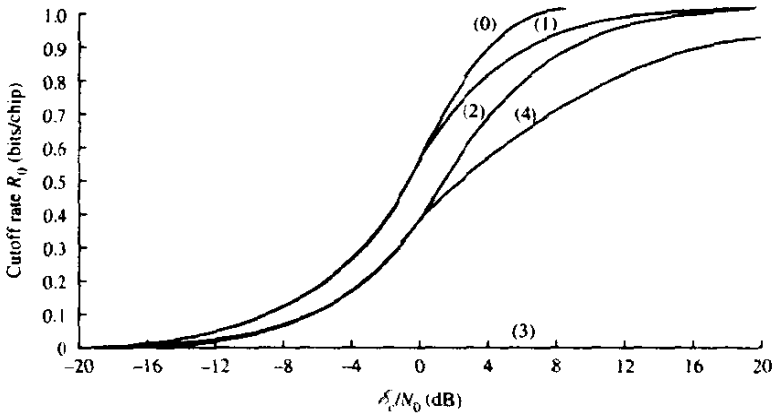

Key
(0) Soft-decision decoding in AWGN ($\alpha \neq 1$)
(1) Soft-decision with jammer state information
(2) Hard-decision with jammer state information
(3) Soft-decision with no jammer state information
(4) Hard-decision with no jammer state information

FIGURE 13-2-13 Cutoff rate for coded DS binary PSK modulation. [*From Omura and Levitt (1982).* © *1982 IEEE.*]

where the probability of error for hard-decision decoding of binary PSK is

$$p = Q\left(\sqrt{\frac{2\alpha\mathscr{E}_c}{N_0}}\right)$$

The graphs for R_0 as a function of $\mathscr{E}_c/N_0$ are illustrated in Fig. 13-2-13 for the cases given above. Note that these graphs represent the cutoff rate for the worst-case value of $\alpha = \alpha^*$ that maximizes D_α (minimizes R_0) for each value of $\mathscr{E}_c/N_0$. Furthermore, note that with soft-decision decoding and no knowledge of the jammer state, $R_0 = 0$. This situation results from the fact that the demodulator output is not quantized.

The graphs in Fig. 13-2-13 may be used to evaluate the performance of coded systems. To demonstrate the procedure, suppose that we wish to determine the SNR required to achieve an error probability of 10^{-6} with coded binary PSK in worst-case pulse jamming. To be specific, we assume that we have a rate 1/2, $K = 7$ convolutional code. We begin with the performance of the rate 1/2, $K = 7$ convolutional code with soft-decision decoding in an AWGN channel. At $P_2 = 10^{-6}$, the SNR required is found from Fig. 8-2-21 to be

$$\mathscr{E}_b/N_0 = 5 \text{ dB}$$

Since the code is rate 1/2, we have

$$\mathscr{E}_c/N_0 = 2 \text{ dB}$$

Now, we go to the graphs in Fig. 13-2-13 and find that for the AWGN channel (reference system) with $\mathscr{E}_c/N_0 = 2$ dB, the corresponding value of the cutoff rate is

$$R_0 = 0.74 \text{ bits/symbol}$$

If we have another channel with different noise characteristics (a worst-case pulse noise channel) but with the same value of the cutoff rate R_0, then the upper bound on the bit error probability is the same, i.e., 10^{-6} in this case. Consequently, we can use this rate to determine the SNR required for the worst-case pulse jammer channel. From the graphs in Fig. 13-2-13, we find that

$$\frac{\mathscr{E}_c}{J_0} = \begin{cases} 10 \text{ dB} & \text{for hard-decision decoding with no knowledge of jammer state} \\ 5 \text{ dB} & \text{for hard-decision decoding with knowledge of jammer state} \\ 3 \text{ dB} & \text{for soft-decision decoding with knowledge of jammer state} \end{cases}$$

Therefore, the corresponding values of $\mathscr{E}_b/J_0$ for the rate 1/2, $K = 7$ convolutional are 13, 8, and 6 dB, respectively.

This general approach may be used to generate error rate graphs for coded binary signals in a worst-case pulse jamming channel by using corresponding error rate graphs for the AWGN channel. The approach we describe above is easily generalized to M-ary coded signals as indicated by Omura and Levitt (1982).

By comparing the cutoff rate for coded DS binary PSK modulation shown in Fig. 13-2-13, we note that for rates below 0.7, there is no penalty in SNR with soft-decision decoding and jammer state information compared with the performance on the AWGN channel ($\alpha = 1$). On the other hand, at $R_0 = 0.7$, there is a 6 dB difference in performance between the SNR in an AWGN channel and that required for hard-decision decoding with no jammer state information. At rates below 0.4, there is no penalty in SNR with hard-decision decoding if the jammer state is unknown. However, there is the expected 2 dB loss in hard-decision decoding compared with soft-decision decoding in the AWGN channel.

13-2-4 Generation of PN Sequences

The generation of PN sequences for spread spectrum applications is a topic that has received considerable attention in the technical literature. We shall briefly discuss the construction of some PN sequences and present a number of important properties of the autocorrelation and cross-correlation functions of such sequences. For a comprehensive treatment of this subject, the interested reader may refer to the book by Golomb (1967).

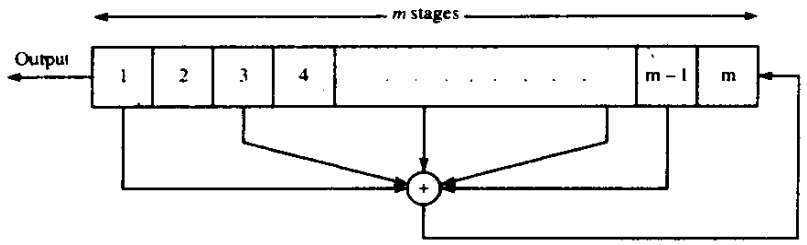

FIGURE 13-2-14 General m-stage shift register with linear feedback.

By far the most widely known binary PN sequences are the maximum-length shift-register sequences introduced in Section 8-1-3 in the context of coding and suggested again in Section 13-2-2 for use as low-rate codes. A maximum-length shift-register sequence, or m-sequence for short, has length $n = 2^m - 1$ bits and is generated by an m-stage shift register with linear feedback as illustrated in Fig. 13-2-14. The sequence is periodic with period n. Each period of the sequence contains 2^{m-1} ones and $2^{m-1} - 1$ zeros.

In DS spread spectrum applications the binary sequence with elements $\{0, 1\}$ is mapped into a corresponding sequence of positive and negative pulses according to the relation

$$p_i(t) = (2b_i - 1)p(t - iT)$$

where $p_i(t)$ is the pulse corresponding to the element b_i in the sequence with elements $\{0, 1\}$. Equivalently, we may say that the binary sequence with elements $\{0, 1\}$ is mapped into a corresponding binary sequence with elements $\{-1, 1\}$. We shall call the equivalent sequence with elements $\{-1, 1\}$ a *bipolar sequence*, since it results in pulses of positive and negative amplitudes.

An important characteristic of a periodic PN sequence is its periodic autocorrelation function, which is usually defined in terms of the bipolar sequence as

$$\phi(j) = \sum_{i=1}^{n} (2b_i - 1)(2b_{i+j} - 1), \qquad 0 \leq j \leq n - 1 \tag{13-2-71}$$

where n is the period. Clearly, $\phi(j + rn) = \phi(j)$ for any integer value r.

Ideally, a pseudo-random sequence should have an autocorrelation function with the property that $\phi(0) = n$ and $\phi(j) = 0$ for $1 \leq j \leq n - 1$. In the case of m sequences, the periodic autocorrelation function is

$$\phi(j) = \begin{cases} n & (j = 0) \\ -1 & (1 \leq j \leq n - 1) \end{cases} \tag{13-2-72}$$

For large values of n, i.e., for long m sequences, the size of the off-peak values of $\phi(j)$ relative to the peak value $\phi(j)/\phi(0) = -1/n$ is small and, from a practical viewpoint, inconsequential. Therefore, m sequences are almost ideal when viewed in terms of their autocorrelation function.

In antijamming applications of PN spread spectrum signals, the period of the sequence must be large in order to prevent the jammer from learning the feedback connections of the PN generator. However, this requirement is impractical in most cases because the jammer can determine the feedback connections by observing only $2m$ chips from the PN sequence. This vulnerability of the PN sequence is due to the linearity property of the generator. To reduce the vulnerability to a jammer, the output sequences from several stages of the shift register or the outputs from several distinct m sequences are combined in a nonlinear way to produce a nonlinear sequence that is considerably more difficult for the jammer to learn. Further reduction in vulnerability is achieved by frequently changing the feedback connections and/or the number of stages in the shift register according to some prearranged plan formulated between the transmitter and the intended receiver.

In some applications, the cross-correlation properties of PN sequences are as important as the autocorrelation properties. For example, in CDMA, each user is assigned a particular PN sequence. Ideally, the PN sequences among users should be mutually orthogonal so that the level of interference experienced by any one user from transmissions of other users adds on a power basis. However, the PN sequences used in practice exhibit some correlation.

To be specific, we consider the class of m sequences. It is known (Sarwate and Pursley, 1980) that the periodic cross-correlation function between any pair of m sequences of the same period can have relatively large peaks. Table 13-2-1 lists the peak magnitude $\phi_{\max}$ for the periodic cross-correlation between pairs of m sequences for $3 \leq m \leq 12$. The table also shows the number of m sequences of length $n = 2^m - 1$ for $3 \leq m \leq 12$. As we can see, the number of m sequences of length n increases rapidly with m. We also observe that, for most sequences, the peak magnitude $\phi_{\max}$ of the cross-correlation function is a large percentage of the peak value of the autocorrelation function.

Such high values for the cross-correlations are undesirable in CDMA.

TABLE 13-2-1 PEAK CROSS-CORRELATION OF m SEQUENCES AND GOLD SEQUENCES

m	$n = 2^m - 1$	Number of m sequences	Peak cross-correlation $\phi_{\max}$	$\phi_{\max}/\phi(0)$	$t(m)$	$t(m)/\phi(0)$
3	7	2	5	0.71	5	0.71
4	15	2	9	0.60	9	0.60
5	31	6	11	0.35	9	0.29
6	63	6	23	0.36	17	0.27
7	127	18	41	0.32	17	0.13
8	255	16	95	0.37	33	0.13
9	511	48	113	0.22	33	0.06
10	1023	60	383	0.37	65	0.06
11	2047	176	287	0.14	65	0.03
12	4095	144	1407	0.34	129	0.03

Although it is possible to select a small subset of m sequences that have relatively smaller cross-correlation peak values, the number of sequences in the set is usually too small for CDMA applications.

PN sequences with better periodic cross-correlation properties than m sequences have been given by Gold (1967, 1968) and Kasami (1966). They are derived from m sequences as described below.

Gold and Kasami proved that certain pairs of m sequences of length n exhibit a three-valued cross-correlation function with values $\{-1, -t(m), t(m)-2\}$, where

$$t(m) = \begin{cases} 2^{(m+1)/2} + 1 & (\text{odd } m) \\ 2^{(m+2)/2} + 1 & (\text{even } m) \end{cases} \tag{13-2-73}$$

For example, if $m = 10$ then $t(10) = 2^6 + 1 = 65$ and the three possible values of the periodic cross-correlation function are $\{-1, -65, 63\}$. Hence the maximum cross-correlation for the pair of m sequences is 65, while the peak for the family of 60 possible sequences generated by a 10-stage shift register with different feedback connections is $\phi_{\max} = 383$—about a sixfold difference in peak values. Two m sequences of length n with a periodic cross-correlation function that takes on the possible values $\{-1, -t(m), t(m)-2\}$ are called *preferred sequences.*

From a pair of preferred sequences, say $\mathbf{a} = [a_1 a_2 \ldots a_n]$ and $\mathbf{b} = [b_1 b_2 \ldots b_n]$, we construct a set of sequences of length n by taking the modulo-2 sum of $\mathbf{a}$ with the n cyclicly shifted versions of $\mathbf{b}$ or vice versa. Thus, we obtain n new periodic sequences† with period $n = 2^m - 1$. We may also include the original sequences $\mathbf{a}$ and $\mathbf{b}$ and, thus, we have a total of $n + 2$ sequences. The $n + 2$ sequences constructed in this manner are called *Gold sequences.*

Example 13-2-4

Let us consider the generation of Gold sequences of length $n = 31 = 2^5 - 1$. As indicated above for $m = 5$, the cross-correlation peak is

$$t(5) = 2^3 + 1 = 9$$

Two preferred sequences, which may be obtained from Peterson and Weldon (1972), are described by the polynomials

$$g_1(p) = p^5 + p^2 + 1$$
$$g_2(p) = p^5 + p^4 + p^2 + p + 1$$

† An equivalent method for generating the n new sequences is to employ a shift register of length $2m$ with feedback connections specified by the polynomial $h(p) = g_1(p)g_2(p)$, where $g_1(p)$ and $g_2(p)$ are the polynomials that specify the feedback connections of the m-stage shift registers that generate the m sequences $\mathbf{a}$ and $\mathbf{b}$.

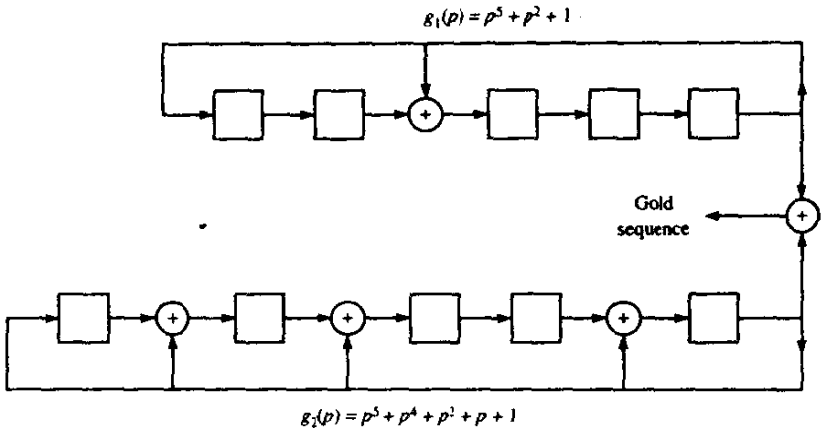

FIGURE 13-2-15 *Generation of Gold sequences of length 31.*

The shift registers for generating the two m sequences and the corresponding Gold sequences are shown in Fig. 13-2-15. In this case, there are 33 different sequences, corresponding to the 33 relative phases of the two m sequences. Of these, 31 sequences are non-maximal-length sequences.

With the exception of the sequences **a** and **b**, the set of Gold sequences does not comprise maximum-length shift-register sequences of length n. Hence, their autocorrelation functions are not two-valued. Gold (1968) has shown that the cross-correlation function for any pair of sequences from the set of $n+2$ Gold sequences is three-valued with possible values $\{-1, -t(m), t(m)-2\}$, where $t(m)$ is given by (13-2-73). Similarly, the off-peak autocorrelation function for a Gold sequence takes on values from the set $\{-1, -t(m), t(m)-2\}$. Hence, the off-peak values of the autocorrelation function are upper-bounded by $t(m)$.

The values of the off-peak autocorrelation function and the peak cross-correlation function, i.e., $t(m)$, for Gold sequences is listed in Table 13-2-1. Also listed are the values normalized by $\phi(0)$.

It is interesting to compare the peak cross-correlation value of Gold sequences with a known lower bound on the cross-correlation between any pair of binary sequences of period n in a set of M sequences. A lower bound developed by Welch (1974) for ϕ_{max} is

$$\phi_{max} \geq n\sqrt{\frac{M-1}{Mn-1}} \tag{13-2-74}$$

which, for large values of n and M, is well approximated as $\sqrt{n}$. For Gold sequences, $n = 2^m - 1$ and, hence, the lower bound is $\phi_{max} \approx 2^{m/2}$. This bound is lower by $\sqrt{2}$ for odd m and by 2 for even m relative to $\phi_{max} = t(m)$ for Gold sequences.

A procedure similar to that used for generating Gold sequences will generate a smaller set of $M = 2^{m/2}$ binary sequences of period $n = 2^m - 1$, where m is even. In this procedure, we begin with an m sequence **a** and we form a binary sequence **b** by taking every $2^{m/2} + 1$ bit of **a**. Thus, the sequence **b** is formed by decimating **a** by $2^{m/2} + 1$. It can be verified that the resulting **b** is periodic with period $2^{m/2} - 1$. For example, if $m = 10$, the period of **a** is $n = 1023$ and the period of **b** is 31. Hence, if we observe 1023 bits of the sequence **b**, we shall see 33 repetitions of the 31-bit sequence. Now, by taking $n = 2^m - 1$ bits of the sequences **a** and **b**, we form a new set of sequences by adding, modulo-2, the bits from **a** and the bits from **b** and all $2^{m/2} - 2$ cyclic shifts of the bits from **b**. By including **a** in the set, we obtain a set of $2^{m/2}$ binary sequences of length $n = 2^m - 1$. These are called *Kasami sequences*. The autocorrelation and cross-correlation functions of these sequences take on values from the set $\{-1, -(2^{m/2} + 1), 2^{m/2} - 1\}$. Hence, the maximum cross-correlation value for any pair of sequences from the set is

$$\phi_{\max} = 2^{m/2} + 1 \tag{13-2-75}$$

This value of $\phi_{\max}$ satisfies the Welch lower bound for a set of $2^{m/2}$ sequences of length $n = 2^m - 1$. Hence, the Kasami sequences are optimal.

Besides the well-known Gold and Kasami sequences, there are other binary sequences appropriate for CDMA applications. The interested reader may refer to the work of Scholtz (1979), Olsen (1977), and Sarwate and Pursley (1980).

Finally, we wish to indicate that, although we have discussed the periodic cross-correlation function between pairs of periodic sequences, many practical CDMA systems may use information bit durations that encompass only fractions of a periodic sequence. In such cases, it is the partial-period cross-correlation between two sequences that is important. A number of papers deal with this problem, including those by Lindholm (1968), Wainberg and Wolf (1970), Fredricsson (1975), Bekir *et al.* (1978), and Pursley (1979).

13-3 FREQUENCY-HOPPED SPREAD SPECTRUM SIGNALS

In a *frequency-hopped* (FH) spread spectrum communications system the available channel bandwidth is subdivided into a large number of contiguous frequency slots. In any signaling interval, the transmitted signal occupies one or more of the available frequency slots. The selection of the frequency slot(s) in each signaling interval is made pseudo-randomly according to the output from a PN generator. Figure 13-3-1 illustrates a particular frequency-hopped pattern in the time-frequency plane.

A block diagram of the transmitter and receiver for a frequency-hopped spread spectrum system is shown in Fig. 13-3-2. The modulation is usually either binary or M-ary FSK. For example, if binary FSK is employed, the modulator selects one of two frequencies corresponding to the transmission of

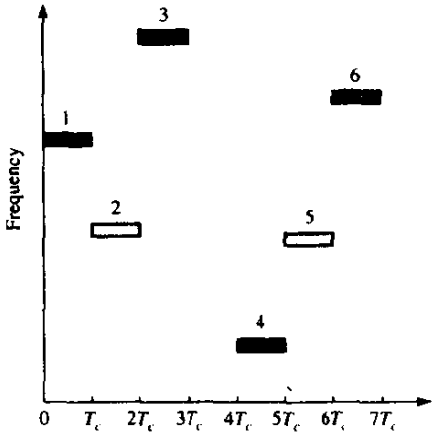

FIGURE 13-3-1 An example of a frequency-hopped (FH) pattern.

either a 1 or a 0. The resulting FSK signal is translated in frequency by an amount that is determined by the output sequence from the PN generator, which, in turn, is used to select a frequency that is synthesized by the frequency synthesizer. This frequency is mixed with the output of the modulator and the resultant frequency-translated signal is transmitted over the channel. For example, m bits from the PN generator may be used to specify $2^m - 1$ possible frequency translations.

At the receiver, we have an identical PN generator, synchronized with the received signal, which is used to control the output of the frequency synthesizer. Thus, the pseudo-random frequency translation introduced at the transmitter is removed at the receiver by mixing the synthesizer output with the received signal. The resultant signal is demodulated by means of an FSK demodulator. A signal for maintaining synchronism of the PN generator with the frequency-translated received signal is usually extracted from the received signal.

Although PSK modulation gives better performance than FSK in an

FIGURE 13-3-2 Block diagram of a FH spread spectrum system.

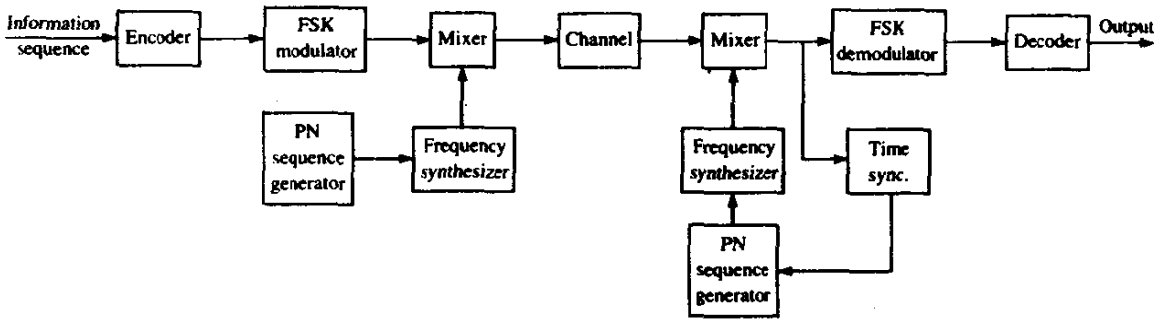

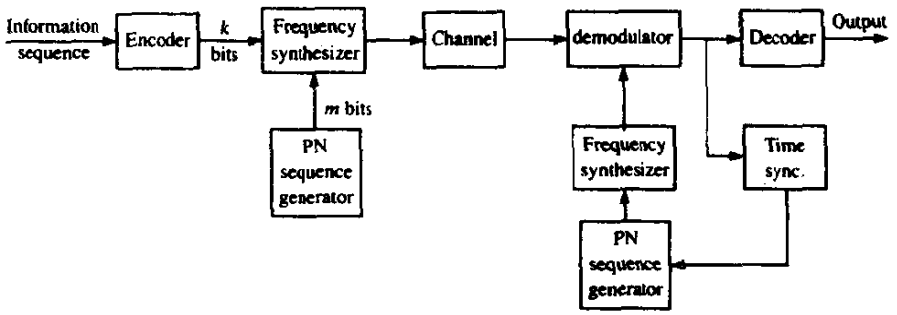

FIGURE 13-3-3 Block diagram of an independent tone FH spread spectrum system.

AWGN channel, it is difficult to maintain phase coherence in the synthesis of the frequencies used in the hopping pattern and, also, in the propagation of the signal over the channel as the signal is hopped from one frequency to another over a wide bandwidth. Consequently, FSK modulation with noncoherent detection is usually employed with FH spread spectrum signals.

In the frequency-hopping system depicted in Fig. 13-3-2, the carrier frequency is pseudo-randomly hopped in every signaling interval. The M information-bearing tones are contiguous and separated in frequency by $1/T_c$, where T_c is the signaling interval. This type of frequency hopping is called *block hopping.*

Another type of frequency hopping that is less vulnerable to some jamming strategies is independent tone hopping. In this scheme, the M possible tones from the modulator are assigned widely dispersed frequency slots. One method for accomplishing this is illustrated in Fig. 13-3-3. Here, the m bits from the PN generator and the k information bits are used to specify the frequency slots for the transmitted signal.

The frequency-hopping rate is usually selected to be either equal to the (coded or uncoded) symbol rate or faster than that rate. If there are multiple hops per symbol, we have a fast-hopped signal. On the other hand, if the hopping is performed at the symbol rate, we have a slow-hopped signal.

Fast frequency hopping is employed in AJ applications when it is necessary to prevent a type of jammer, called a *follower jammer,* from having sufficient time to intercept the frequency and retransmit it along with adjacent frequencies so as to create interfering signal components. However, there is a penalty incurred in subdividing a signal into several frequency-hopped elements because the energy from these separate elements is combined noncoherently. Consequently, the demodulator incurs a penalty in the form of a noncoherent combining loss as described in Section 12-1.

FH spread spectrum signals are used primarily in digital communications systems that require AJ projection and in CDMA, where many users share a common bandwidth. In most cases, a FH signal is preferred over a DS spread spectrum signal because of the stringent synchronization requirements

inherent in DS spread spectrum signals. Specifically, in a DS system, timing and synchronization must be established to within a fraction of the chip interval $T_c \approx 1/W$. On the other hand, in an FH system, the chip interval is the time spent in transmitting a signal in a particular frequency slot of bandwidth $B \ll W$. But this interval is approximately $1/B$, which is much larger than $1/W$. Hence the timing requirements in a FH system are not as stringent as in a PN system.

In Sections 13-3-2 and 13-3-3, we shall focus on the AJ and CDMA applications of FH spread spectrum signals. First, we shall determine the error rate performance of an uncoded and a coded FH signal in the presence of broadband AWGN interference. Then we shall consider a more serious type of interference that arises in AJ and CDMA applications, called *partial-band interference*. The benefits obtained from coding for this type of interference are determined. We conclude the discussion in Section 13-3-3 with an example of an FH CDMA system that was designed for use by mobile users with a satellite serving as the channel.

13-3-1 Performance of FH Spread Spectrum Signals in AWGN Channel

Let us consider the performance of a FH spread spectrum signal in the presence of broadband interference characterized statistically as AWGN with power spectral density J_0. For binary orthogonal FSK with noncoherent detection and slow frequency hopping (1 hop/bit), the probability of error, derived in Section 5-4-1, is

$$P_2 = \tfrac{1}{2} e^{-\gamma_b/2} \tag{13-3-1}$$

where $\gamma_b = \mathscr{E}_b/J_0$. On the other hand, if the bit interval is subdivided into L subintervals and FH binary FSK is transmitted in each subinterval, we have a fast FH signal. With square-law combining of the output signals from the corresponding matched filters for the L subintervals, the error rate performance of the FH signal, obtained from the results in Section 12-1, is

$$P_2(L) = \frac{1}{2^{2L-1}} e^{-\gamma_b/2} \sum_{i=0}^{L-1} K_i (\tfrac{1}{2}\gamma_b)^i \tag{13-3-2}$$

where the SNR per bit is $\gamma_b = \mathscr{E}_b/J_0 = L\gamma_c$, γ_c is the SNR per chip in the L-chip symbol, and

$$K_i = \frac{1}{i!} \sum_{r=0}^{L-1-i} \binom{2L-1}{r} \tag{13-3-3}$$

We recall that, for a given SNR per bit γ_b, the error rate obtained from (13-3-2) is larger than that obtained from (13-3-1). The difference in SNR for a given error rate and a given L is called the *noncoherent combining loss*, which was described and illustrated in Section 12-1.

Coding improves the performance of the FH spread spectrum system by an

amount, which we call the *coding gain*, that depends on the code parameters. Suppose we use a linear binary (n, k) block code and binary FSK modulation with one hop per coded bit for transmitting the bits. With soft-decision decoding of the square-law -demodulated FSK signal, the probability of a code word error is upper-bounded as

$$P_M \leq \sum_{m=2}^{M} P_2(m) \tag{13-3-4}$$

where $P_2(m)$ is the error probability in deciding between the mth code word and the all-zero code word when the latter has been transmitted. The expression for $P_2(m)$ was derived in Section 8-1-4 and has the same form as (13-3-2) and (13-3-3), with L being replaced by w_m and γ_b by $\gamma_b R_c w_m$, where w_m is the weight of the mth code word and R_c is the code rate. The product $R_c w_m$, which is not less than $R_c d_{\min}$, represents the coding gain. Thus, we have the performance of a block coded FH system with slow frequency hopping in broadband interference.

The probability of error for fast frequency hopping with n_2 hops per coded bit is obtained by reinterpreting the binary event probability $P_2(m)$ in (13-3-4). The n_2 hops per coded bit may be interpreted as a repetition code, which, when combined with a nontrivial (n_1, k) binary linear code having weight distribution $\{w_m\}$, yields an $(n_1 n_2, k)$ binary linear code with weight distribution $\{n_2 w_m\}$. Hence, $P_2(m)$ has the form given in (13-3-2), with L replaced by $n_2 w_m$ and γ_b by $\gamma_b R_c n_2 w_m$, where $R_c = k/n_1 n_2$. Note that $\gamma_b R_c n_2 w_m = \gamma_b w_m k/n_1$, which is just the coding gain obtained from the nontrivial (n_1, k) code. Consequently, the use of the repetition code will result in an increase in the noncoherent combining loss.

With hard-decision decoding and slow frequency hopping, the probability of a coded bit error at the output of the demodulator for noncoherent detection is

$$p = \tfrac{1}{2} e^{-\gamma_b R_c/2} \tag{13-3-5}$$

The code word error probability is easily upper-bounded, by use of the Chernoff bound, as

$$P_M \leq \sum_{m=2}^{M} [4p(1-p)]^{w_m/2} \tag{13-3-6}$$

However, if fast frequency hopping is employed with n_2 hops per coded bit, and the square-law-detected outputs from the corresponding matched filters for the n_2 hops are added as in soft-decision decoding to form the two decision variables for the coded bits, the bit error probability p is also given by (13-3-2), with L replaced by n_2 and γ_b replaced by $\gamma_b R_c n_2$, where R_c is the rate of the nontrivial (n_1, k) code. Consequently, the performance of the fast FH system in broadband interference is degraded relative to the slow FH system by an amount equal to the noncoherent combining loss of the signals received from the n_2 hops.

We have observed that for both hard-decision and soft-decision decoding, the use of the repetition code in a fast-frequency-hopping system yields no coding gain. The only coding gain obtained comes from the (n_1, k) block code. Hence, the repetition code is inefficient in a fast FH system with noncoherent combining. A more efficient coding method is one in which either a single low-rate binary code or a concatenated code is employed. Additional improvements in performance may be obtained by using nonbinary codes in conjunction with M-ary FSK. Bounds on the error probability for this case may be obtained from the results given in Section 12-1.

Although we have evaluated the performance of linear block codes only in the above discussion, it is relatively easy to derive corresponding performance results for binary convolutional codes. We leave as an exercise for the reader the derivation of the bit error probability for soft-decision Viterbi decoding and hard-decision Viterbi decoding of FH signals corrupted by broadband interference.

Finally, we observe that $\mathcal{E}_b$, the energy per bit, can be expressed as $\mathcal{E}_b = P_{av}/R$, where R is the information rate in bits per second and $J_0 = J_{av}/W$. Therefore, γ_b may be expressed as

$$\gamma_b = \frac{\mathcal{E}_b}{J_0} = \frac{W/R}{J_{av}/P_{av}} \tag{13-3-7}$$

In this expression, we recognize W/R as the processing gain and J_{av}/P_{av} as the jamming margin for the FH spread spectrum signal.

13-3-2 Performance of FH Spread Spectrum Signals in Partial-Band Interference

The partial-band interference considered in this subsection is modeled as a zero-mean gaussian random process with a flat power spectral density over a fraction α of the total bandwidth W and zero elsewhere. In the region or regions where the power spectral density is nonzero, its value is $\Phi_{zz}(f) = J_0/\alpha$, $0 < \alpha \leq 1$. This model of the interference may be applied to a jamming signal or to interference from other users in a FH CDMA system.

Suppose that the partial-band interference comes from a jammer who may select α to optimize the effect on the communications system. In an uncoded pseudo-randomly hopped (slow-hopping) FH system with binary FSK modulation and noncoherent detection, the received signal will be jammed with probability α and it will not be jammed with probability $1 - \alpha$. When it is jammed, the probability of error is $\frac{1}{2}\exp(-\mathcal{E}_b\alpha/2J_0)$, and when it is not jammed, the demodulation is error-free. Consequently, the average probability of error is

$$P_2(\alpha) = \tfrac{1}{2}\alpha \exp\left(-\frac{\alpha\mathcal{E}_b}{2J_0}\right) \tag{13-3-8}$$

where $\mathcal{E}_b/J_0$ may also be expressed as $(W/R)/(J_{av}/P_{av})$.

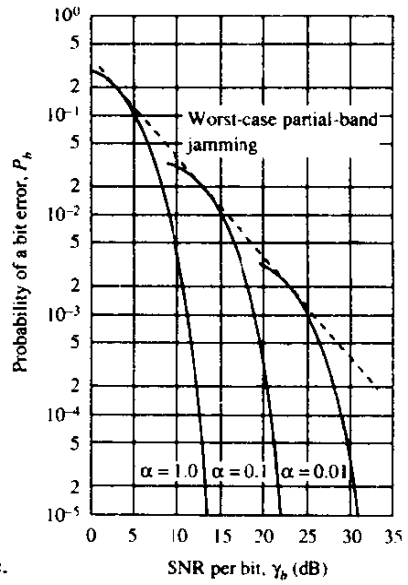

FIGURE 13-3-4 Performance of binary FSK with partial-band interference.

Figure 13-3-4 illustrates the error rate as a function of $\mathscr{E}_b/J_0$ for several values of α. The jammer's optimum strategy is to select the value of α that maximizes the error probability. By differentiating $P_2(\alpha)$ and solving for the extremum with the restriction that $0 \leq \alpha \leq 1$, we find that

$$\alpha^* = \begin{cases} \dfrac{1}{\mathscr{E}_b/2J_0} = 2\dfrac{J_{av}/P_{av}}{W/R} & (\mathscr{E}_b/J_0 \geq 2) \\ 1 & (\mathscr{E}_b/J_0 < 2) \end{cases} \tag{13-3-9}$$

The corresponding error probability for the worst-case partial-band jammer is

$$P_2 = \frac{e^{-1}}{\mathscr{E}_b/J_0} = \left[e\left(\frac{W/R}{J_{av}/P_{av}}\right)\right]^{-1} \tag{13-3-10}$$

Whereas the error probability decreases exponentially for full-band jamming, we now find that the error probability decreases only inversely with $\mathscr{E}_b/J_0$ for the worst-case partial-band jamming. This result is similar to the error rate performance of binary FSK in a Rayleigh fading channel (see Section 14-3) and to the uncoded DS spread spectrum system corrupted by worst-case pulse jamming (see Section 13-2-3).

As we shall demonstrate below, signal diversity obtained by means of coding provides a significant improvement in performance relative to uncoded signals. This same approach to signal design is also effective for signaling over a fading channel, as we shall demonstrate in Chapter 14.

To illustrate the benefits of diversity in a FH spread spectrum signal with partial-band interference, we assume that the same information symbol is

transmitted by binary FSK on L independent frequency hops. This may be accomplished by subdividing the signaling interval into L subintervals, as described previously for fast frequency hopping. After the hopping pattern is removed, the signal is demodulated by passing it through a pair of matched filters whose outputs are square-law-detected and sampled at the end of each subinterval. The square-law-detected signals corresponding to the L frequency hops are weighted and summed to form the two decision variables (metrics), which are denoted as U_1 and U_2.

When the decision variable U_1 contains the signal components, U_1 and U_2 may be expressed as

$$\begin{aligned} U_1 &= \sum_{k=1}^{L} \beta_k |2\mathscr{E}_c + N_{1k}|^2 \\ U_2 &= \sum_{k=1}^{L} \beta_k |N_{2k}|^2 \end{aligned} \tag{13-3-11}$$

where $\{\beta_k\}$ represent the weighting coefficients, $\mathscr{E}_c$ is the signal energy per chip in the L-chip symbol, and $\{N_{jk}\}$ represent the additive gaussian noise terms at the output of the matched filters.

The coefficients are optimally selected to prevent the jammer from saturating the combiner should the transmitted frequencies be successfully hit in one or more hops. Ideally, β_k is selected to be equal to the reciprocal of the variance of the corresponding noise terms $\{N_k\}$. Thus, the noise variance for each chip is normalized to unity by this weighting and the corresponding signal is also scaled accordingly. This means that when the signal frequencies on a particular hop are jammed, the corresponding weight is very small. In the absence of jamming on a given hop, the weight is relatively large. In practice, for partial-bound noise jamming, the weighting may be accomplished by use of an AGC having a gain that is set on the basis of noise power measurements obtained from frequency bands adjacent to the transmitted tones. This is equivalent to having side information (knowledge of jammer state) at the decoder.

Suppose that we have broadband gaussian noise with power spectral density N_0 and partial-band interference, over αW of the frequency band, which is also gaussian with power spectral density J_0/α. In the presence of partial-band interference, the second moments of the noise terms N_{1k} and N_{2k} are

$$\sigma_k^2 = \tfrac{1}{2}E(|N_{1k}|^2) = \tfrac{1}{2}E(|N_{2k}|^2) = 2\mathscr{E}_c\left(N_0 + \frac{J_0}{\alpha}\right) \tag{13-3-12}$$

In this case, we select $\beta_k = 1/\sigma_k^2 = [2\mathscr{E}_c(N_0 + J_0/\alpha)]^{-1}$. In the absence of partial-band interference, $\sigma_k^2 = 2\mathscr{E}_c N_0$ and, hence, $\beta_k = (2\mathscr{E}_c N_0)^{-1}$. Note that β_k is a random variable.

An error occurs in the demodulation if $U_2 > U_1$. Although it is possible to determine the exact error probability, we shall resort to the Chernoff bound,

which yields a result that is much easier to evaluate and interpret. Specifically, the Chernoff (upper) bounds in the error probability is

$$\begin{aligned} P_2 &= P(U_2 - U_1 > 0) \leq E\{\exp[\nu(U_2 - U_1)]\} \\ &= E\left\{\exp\left[-\nu \sum_{k=1}^{L} \beta_k (|2\mathscr{E}_c + N_{1k}|^2 - |N_{2k}|^2)\right]\right\} \end{aligned} \tag{13-3-13}$$

where ν is a variable that is optimized to yield the tightest possible bound.

The averaging in (13-3-13) is performed with respect to the statistics of the noise components and the statistics of the weighting coefficients $\{\beta_k\}$, which are random as a consequence of the statistical nature of the interference. Keeping the $\{\beta_k\}$ fixed and averaging over the noise statistics first, we obtain

$$\begin{aligned} P_2(\boldsymbol{\beta}) &= E\left[\exp\left(-\nu \sum_{k=1}^{L} \beta_k |2\mathscr{E}_c + N_{1k}|^2 + \nu \sum_{k=1}^{L} \beta_k |N_{2k}|^2\right)\right] \\ &= \prod_{k=1}^{L} E[\exp(-\nu\beta_k |2\mathscr{E}_c + N_{1k}|^2)] E[\exp(\nu\beta_k |N_{2k}|^2)] \\ &= \prod_{k=1}^{L} \frac{1}{1-4\nu^2} \exp\left(\frac{-4\mathscr{E}_c^2 \beta_k \nu}{1+2\nu}\right) \end{aligned} \tag{13-3-14}$$

Since the FSK tones are jammed with probability α, it follows that $\beta_k = [2\mathscr{E}(N_0 + J_0/\alpha)]^{-1}$ with probability α and $(2\mathscr{E}_c N_0)^{-1}$ with probability $1-\alpha$. Hence, the Chernoff bound is

$$\begin{aligned} P_2 &\leq \prod_{k=1}^{L} \left\{\frac{\alpha}{1-4\nu^2} \exp\left[\frac{-2\mathscr{E}_c \nu}{(N_0 + J_0/\alpha)(1+2\nu)}\right] + \frac{1-\alpha}{1-4\nu^2} \exp\left[\frac{-2\mathscr{E}_c \nu}{N_0(1+2\nu)}\right]\right\} \\ &= \left\{\frac{\alpha}{1-4\nu^2} \exp\left[\frac{-2\mathscr{E}_c \nu}{(N_0 + J_0/\alpha)(1+2\nu)}\right] + \frac{1-\alpha}{1-4\nu^2} \exp\left[\frac{-2\mathscr{E}_c \nu}{N_0(1+2\nu)}\right]\right\}^L \end{aligned} \tag{13-3-15}$$

The next step is to optimize the bound in (13-3-15) with respect to the variable ν. In its present form, however, the bound is messy to manipulate. A significant simplification occurs if we assume that $J_0/\alpha \gg N_0$, which renders the second term in (13-3-15) negligible compared with the first. Alternatively, we let $N_0 = 0$, so that the bound on P_2 reduces to

$$P_2 \leq \left\{\frac{\alpha}{1-4\nu^2} \exp\left[\frac{-2\alpha\nu\mathscr{E}_c}{J_0(1+2\nu)}\right]\right\}^L \tag{13-3-16}$$

The minimum value of this bound with respect to ν and the maximum with respect to α (worst-case partial-band interference) is easily shown to occur when $\alpha = 3J_0/\mathscr{E}_c \leq 1$ and $\nu = \frac{1}{4}$. For these values of the parameters, (13-3-16) reduces to

$$P_2 \leq P_2(L) = \left(\frac{4}{e\gamma_c}\right)^L = \left(\frac{1.47}{\gamma_c}\right)^L, \qquad \gamma_c = \frac{\mathscr{E}_c}{J_0} = \frac{\mathscr{E}_b}{LJ_0} \geq 3 \tag{13-3-17}$$

where γ_c is the SNR per chip in the L-chip symbol. Equivalently,

$$P_2 \leq \left[\frac{1.47(J_{av}/P_{av})}{W/R}\right]^L, \quad \frac{W/R}{L(J_{av}/P_{av})} \geq 3 \tag{13-3-18}$$

The result in (13-3-17) was first derived by Viterbi and Jacobs (1975).

We observe that the probability of error for the worst-case partial-band interference decreases exponentially with an increase in the SNR per chip γ_c. This result is very similar to the performance characteristics of diversity techniques for Rayleigh fading channels (see Section 14-4). We may express the right-hand side of (13-3-17) in the form

$$P_2(L) = \exp[-\gamma_b h(\gamma_c)] \tag{13-3-19}$$

where the function $h(\gamma_c)$ is defined as

$$h(\gamma_c) = -\frac{1}{\gamma_c}\left[\ln\left(\frac{4}{\gamma_c}\right) - 1\right] \tag{13-3-20}$$

A plot of $h(\gamma_c)$ is given in Fig. 13-3-5. We observe that the function has a maximum value of $\frac{1}{4}$ at $\gamma_c = 4$. Consequently, there is an optimum SNR per chip of $10 \log \gamma_c = 6$ dB. At the optimum SNR, the error rate is upper-bounded as

$$P_2 \leq P_2(L_{opt}) = e^{-\gamma_b/4} \tag{13-3-21}$$

When we compare the error probability bound in (13-3-21) with the error probability for binary FSK in spectrally flat noise, which is given by (13-3-1), we see that the combined effect of worst-case partial-band interference and the noncoherent combining loss in the square-law combining of the L chips is 3 dB. We emphasize, however, that for a given $\mathscr{E}_b/J_0$, the loss is greater when the order of diversity is not optimally selected.

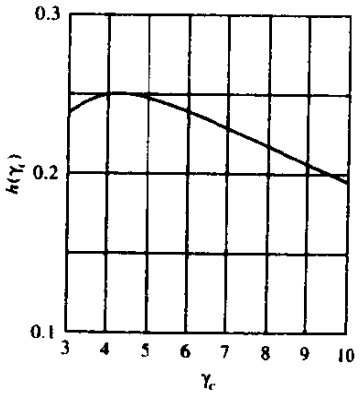

FIGURE 13-3-5 Graph of the function $h(\gamma_c)$.

Coding provides a means for improving the performance of the frequency-hopped system corrupted by partial-band interference. In particular, if a block orthogonal code is used, with $M = 2^k$ code words and Lth-order diversity per code word, the probability of a code word error is upper-bounded as

$$P_M \leq (2^k - 1)P_2(L) = (2^k - 1)\left(\frac{1.47}{\gamma_c}\right)^L = (2^k - 1)\left(\frac{1.47}{k\gamma_b/L}\right)^L \quad (13\text{-}3\text{-}22)$$

and the equivalent bit error probability is upper-bounded as

$$P_b \leq 2^{k-1}\left(\frac{1.47}{k\gamma_b/L}\right)^L \quad (13\text{-}3\text{-}23)$$

Figure 13-3-6 illustrates the probability of a bit error for $L = 1, 2, 4, 8$ and

FIGURE 13-3-6 Performance of binary and octal FSK with L-order diversity for a channel with worst-case partial-band interference.

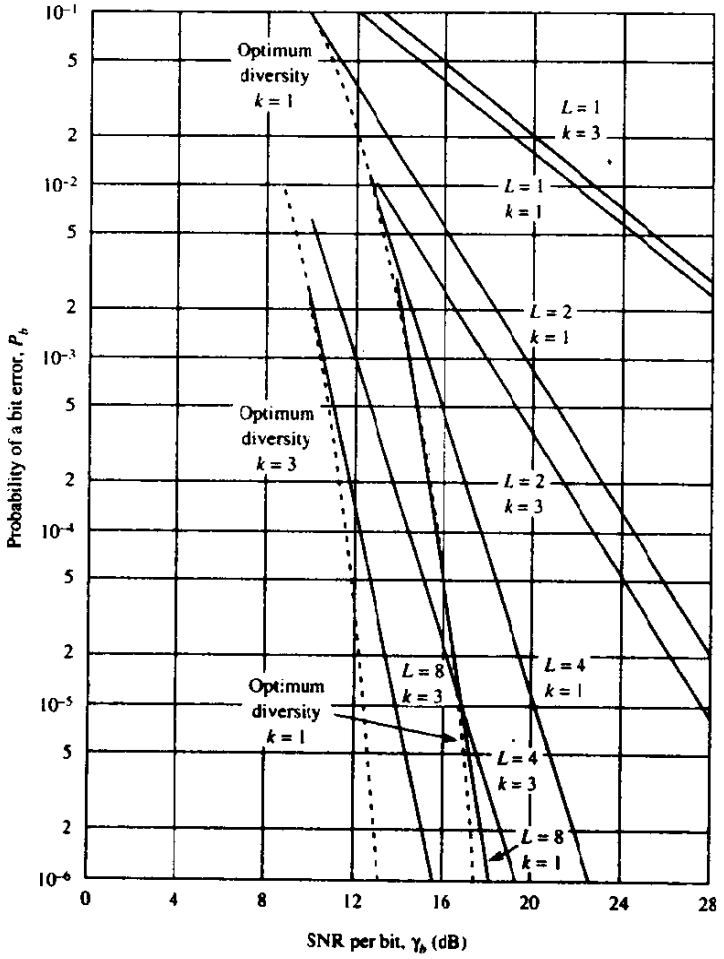

$k = 1, 3$. With an optimum choice of diversity, the upper bound can be expressed as

$$P_b \leq 2^{k-1} \exp(-\tfrac{1}{4}k\gamma_b) = \tfrac{1}{2}\exp[-k(\tfrac{1}{4}\gamma_b - \ln 2)] \qquad (13\text{-}3\text{-}24)$$

Thus, we have an improvement in performance by an amount equal to $10\log[k(1 - 2.77/\gamma_b)]$. For example, if $\gamma_b = 10$ and $k = 3$ (octal modulation) then the gain is 3.4 dB, while if $k = 5$ then the gain is 5.6 dB.

Additional gains can be achieved by employing concatenated codes in conjunction with soft-decision decoding. In the example below, we employ a dual-k convolutional code as the outer code and a Hadamard code as the inner code on the channel with partial-band interference.

Example 13-3-1

Suppose we use a Hadamard $H(n, k)$ constant weight code with on-off keying (OOK) modulation for each code bit. The minimum distance of the code is $d_{\min} = \frac{1}{2}n$, and, hence, the effective order of diversity obtained with OOK modulation is $\frac{1}{2}d_{\min} = \frac{1}{4}n$. There are $\frac{1}{2}n$ frequency-hopped tones transmitted per code word. Hence,

$$\gamma_c = \frac{k}{\frac{1}{2}n}\gamma_b = 2R_c\gamma_b \qquad (13\text{-}3\text{-}25)$$

when this code is used alone. The bit error rate performance for soft-decision decoding of these codes for the partial-band interference channel is upper-bounded as

$$P_b \leq 2^{k-1}P_2(\tfrac{1}{2}d_{\min}) = 2^{k-1}\left(\frac{1.47}{2R_c\gamma_b}\right)^{n/4} \qquad (13\text{-}3\text{-}26)$$

Now, if a Hadamard (n, k) code is used as the inner code and a rate 1/2 dual-k convolutional code (see Section 8-2-6) is the outer code, the bit error performance in the presence of worst-case partial-band interference is (see (8-2-40))

$$P_b \leq \frac{2^{k-1}}{2^k - 1}\sum_{m=4}^{\infty}\beta_m P_2(\tfrac{1}{2}md_{\min}) = \frac{2^{k-1}}{2^k - 1}\sum_{m=4}^{\infty}\beta_m P_2(\tfrac{1}{4}mn) \qquad (13\text{-}3\text{-}27)$$

where $P_2(L)$ is given by (13-3-17) with

$$\gamma_c = \frac{k}{n}\gamma_b = R_c\gamma_b \qquad (13\text{-}3\text{-}28)$$

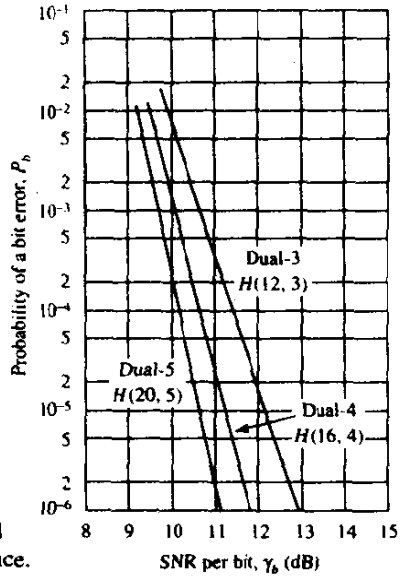

FIGURE 13-3-7 Performance of dual-k codes concatenated with Hadamard codes for a channel with worst-case partial-band interference.

Figure 13-3-7 illustrates the performance of the dual-k codes for $k = 5$, 4, and 3 concatenated with the Hadamard $H(20, 5)$, $H(16, 4)$, and $H(12, 3)$ codes, respectively.

In the above discussion, we have focused on soft-decision decoding. On the other hand, the performance achieved with hard-decision decoding is significantly (several decibels) poorer than that obtained with soft-decision decoding. In a concatenated coding scheme, however, a mixture involving soft-decision decoding of the inner code and hard-decision decoding of the outer code represents a reasonable compromise between decoding complexity and performance.

Finally, we wish to indicate that another serious threat in a FH spread spectrum system is partial-band multitone jamming. This type of interference is similar in effect to partial-band spectrally flat noise jamming. Diversity obtained through coding is an effective means for improving the performance of the FH system. An additional improvement is achieved by properly weighting the demodulator outputs so as to suppress the effects of the jammer.

13-3-3 A CDMA System Based on FH Spread Spectrum Signals

In Section 13-2-2, we considered a CDMA system based on use of DS spread spectrum signals. As previously indicated, it is also possible to have a CDMA system based on FH spread spectrum signals. Each transmitter–receiver pair in such a system is assigned its own pseudo-random frequency-hopping pattern.

Aside from this distinguishing feature, the transmitters and receivers of all the users may be identical in that they may have identical encoders, decoders, modulators, and demodulators.

CDMA systems based on FH spread spectrum signals are particularly attractive for mobile (land, air, sea) users because timing requirements are not as stringent as in a PN spread spectrum signal. In addition, frequency synthesis techniques and associated hardware have been developed that make it possible to frequency-hop over bandwidths that are significantly larger than those currently possible with DS spread spectrum systems. Consequently, larger processing gains are possible with FH. The capacity of CDMA with FH is also relatively high. Viterbi (1978) has shown that with dual-k codes and M-ary FSK modulation, it is possible to accomodate up to $\frac{3}{8}W/R$ simultaneous users who transmit at an information rate R bits/s over a channel with bandwidth W.

One of the earliest CDMA systems based on FH coded spread spectrum signals was built to provide multiple-access tactical satellite communications for small mobile (land, sea, air) terminals each of which transmitted relatively short messages over the channel intermittently. The system was called the *Tactical Transmission System* (TATS) and it is described in a paper by Drouilhet and Bernstein (1969).

An octal Reed–Solomon (7, 2) code is used in the TATS system. Thus, two 3 bit information symbols from the input to the encoder are used to generate a seven-symbol code word. Each 3 bit coded symbol is transmitted by means of octal FSK modulation. The eight possible frequencies are spaced $1/T_c$ Hz apart, where T_c is the time (chip) duration of a single frequency transmission. In addition to the seven symbols in a code word, an eighth symbol is included. That symbol and its corresponding frequency are fixed and transmitted at the beginning of each code word for the purpose of providing timing and frequency synchronization† at the receiver. Consequently, each code word is transmitted in $8T_c$ s.

TATS was designed to transmit at information rates of 75 and 2400 bits/s. Hence, $T_c = 10$ ms and 312.5 μs, respectively. Each frequency tone corresponding to a code symbol is frequency-hopped. Hence, the hopping rate is 100 hops/s at the 75 bits/s rate and 3200 hops/s at the 2400 bits/s rate.

There are $M = 2^6 = 64$ code words in the Reed–Solomon (7, 2) code and the minimum distance of the code is $d_{\min} = 6$. This means that the code provides an effective order of diversity equal to 6.

At the receiver, the received signal is first dehopped and then demodulated by passing it through a parallel bank of eight matched filters, where each filter is tuned to one of the eight possible frquencies. Each filter output is envelope-detected, quantized to 4 bits (one of 16 levels), and fed to the decoder. The decoder takes the 56 filter outputs corresponding to the

† Since mobile users are involved, there is a Doppler frequency offset associated with transmission. This frequency offset must be tracked and compensated for in the demodulation of the signal. The sync symbol is used for this purpose.

reception of each seven-symbol code word and forms 64 decision variables corresponding to the 64 possible code words in the (7, 2) code by linearly combining the appropriate envelope detected outputs. A decision is made in favor of the code word having the largest decision variable.

By limiting the matched filter outputs to 16 levels, interference (crosstalk) from other users of the channel causes a relatively small loss in performance (0.75 dB with strong interference on one chip and 1.5 dB with strong interference on two chips out of the seven). The AGC used in TATS has a time constant greater than the chip interval T_c, so that no attempt is made to perform optimum weighting of the demodulator outputs as described in Section 13-3-2.

The derivation of the error probability for the TATS signal in AWGN and worst-case partial-band interference is left as an exercise for the reader (Problems 13-23 and 13-24).

13-4 OTHER TYPES OF SPREAD SPECTRUM SIGNALS

DS and FH are the most common forms of spread spectrum signals used in practice. However, other methods may be used to introduce pseudo-randomness in a spread spectrum signal. One method, which is analogous to FH, is *time* hopping (TH). In TH, a time interval, which is selected to be much larger than the reciprocal of the information rate, is subdivided into a large number of time slots. The coded information symbols are transmitted in a pseudo-randomly selected time slot as a block of one or more code words. PSK modulation may be used to transmit the coded bits.

For example, suppose that a time interval T is subdivided into 1000 time slots of width $T/1000$ each. With an information bit rate of R bits/s, the number of bits to be transmitted in T s is RT. Coding increases this number to RT/R_c bits, where R_c is the coding rate. Consequently, in a time interval of $T/1000$ s, we must transmit RT/R_c bits. If binary PSK is used as the modulation method, the bit rate is $1000R/R_c$ and the bandwidth required is approximately $W = 1000R/R_c$.

A block diagram of a transmitter and a receiver for a TH spread spectrum system is shown in Fig. 13-4-1. Due to the burst characteristics of the transmitted signal, buffer storage must be provided at the transmitter in a TH system, as shown in Fig. 13-4-1. A buffer may also be used at the receiver to provide a uniform data stream to the user.

Just as partial-band interference degrades an uncoded FH spread spectrum system, partial-time (pulsed) interference has a similar effect on a TH spread spectrum system. Coding and interleaving are effective means for combatting this type of interference, as we have already demonstrated for FH and DS systems. Perhaps the major disadvantage of a TH system is the stringent timing requirements compared not only with FH but, also, with DS.

Other types of spread spectrum signals can be obtained by combining DS,

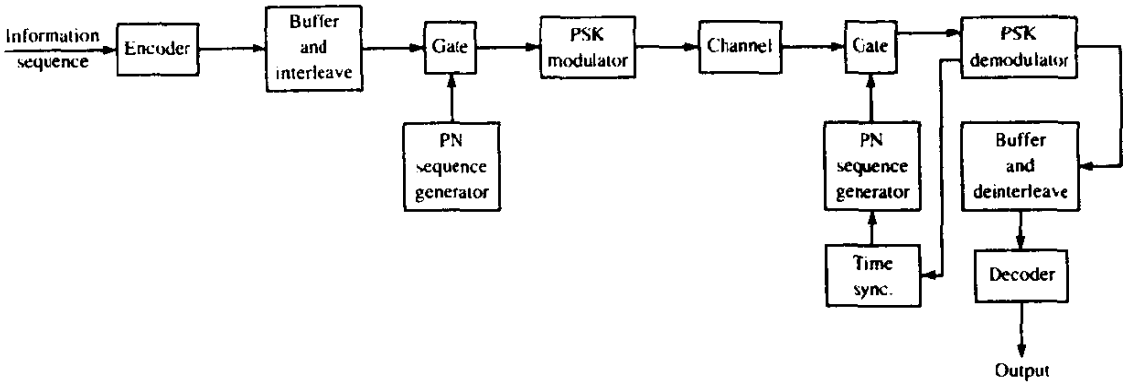

FIGURE 13-4-1 Block diagram of time-hopping (TH) spread spectrum system.

FH, and TH. For example, we may have a hybrid DS/FH, which means that a PN sequence is used in combination with frequency hopping. The signal transmitted on a single hop consists of a DS spread spectrum signal which is demodulated coherently. However, the received signals from different hops are combined noncoherently (envelope or square-law combining). Since coherent detection is performed within a hop, there is an advantage obtained relative to a pure FH system. However, the price paid for the gain in performance is an increase in complexity, greater cost, and more stringent timing requirements.

Another possible hybrid spread spectrum signal is DS/TH. This does not seem to be as practical as DS/FH, primarily because of an increase in system complexity and more stringent timing requirements.

13-5 SYNCHRONIZATION OF SPREAD SPECTRUM SYSTEMS

Time synchronization of the receiver to the received spread spectrum signal may be separated into two phases. There is an initial acquisition phase and a tracking phase after the signal has been initially acquired.

Acquisition In a direct sequence spread spectrum system, the PN code must be time-synchronized to within a small fraction of the chip interval $T_c \approx 1/W$. The problem of initial synchronization may be viewed as one in which we attempt to synchronize in time the receiver clock to the transmitter clock. Usually, extremely accurate and stable time clocks are used in spread spectrum systems. Consequently, accurate time clocks result in a reduction of the time uncertainty between the receiver and the transmitter. However, there is always an initial timing uncertainty due to range uncertainty between the transmitter and the receiver. This is especially a problem when communication is taking place between two mobile users. In any case, the usual procedure for establishing initial synchronization is for the transmitter to send a known

pseudo-random data sequence to the receiver. The receiver is continuously in a search mode looking for this sequence in order to establish initial synchronization.

Let us suppose that the initial timing uncertainty is T_u and the chip duration is T_c. If initial synchronization is to take place in the presence of additive noise and other interference, it is necessary to dwell for $T_d = NT_c$ in order to test synchronism at each time instant. If we search over the time uncertainty interval in (coarse) time steps of $\frac{1}{2}T_c$ then the time required to establish initial synchronization is

$$T_{init\ sync} = \frac{T_u}{\frac{1}{2}T_c} NT_c = 2NT_u \tag{13-5-1}$$

Clearly, the synchronization sequence transmitted to the receiver must be at least as long as $2NT_c$ in order for the receiver to have sufficient time to perform the necessary search in a serial fashion.

In principle, matched filtering or cross-correlation are optimum methods for establishing initial synchronization. A filter matched to the known data waveform generated from the known pseudo-random sequence continuously looks for exceedence of a predetermined threshold. When this occurs, initial synchronization is established and the demodulator enters the "data receive" mode.

Alternatively, we may use a *sliding correlator* as shown in Fig. 13-5-1. The correlator cycles through the time uncertainty, usually in discrete time intervals of $\frac{1}{2}T_c$, and correlates the received signal with the known synchronization sequence. The cross-correlation is performed over the time interval NT_c (N chips) and the correlator output is compared with a threshold to determine if the known signal sequence is present. If the threshold is not exceeded, the known reference sequence is advanced in time by $\frac{1}{2}T_c$ s and the correlation process is repeated. These operations are performed until a signal is detected or until the search has been performed over the time uncertainty interval T_u. In the latter case, the search process is then repeated.

A similar process may also be used for FH signals. In this case, the problem is to synchronize the PN code that controls the hopped frequency pattern. To accomplish this initial synchronization, a known frequency hopped signal is

FIGURE 13-5-1 A sliding correlator for DS signal acquisition.

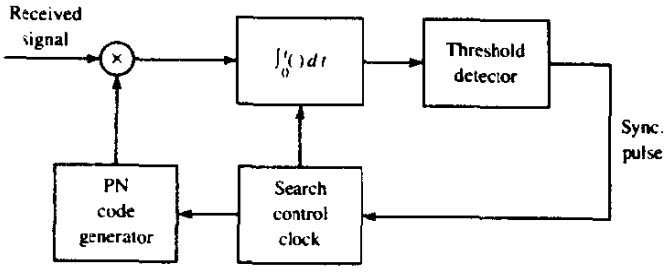

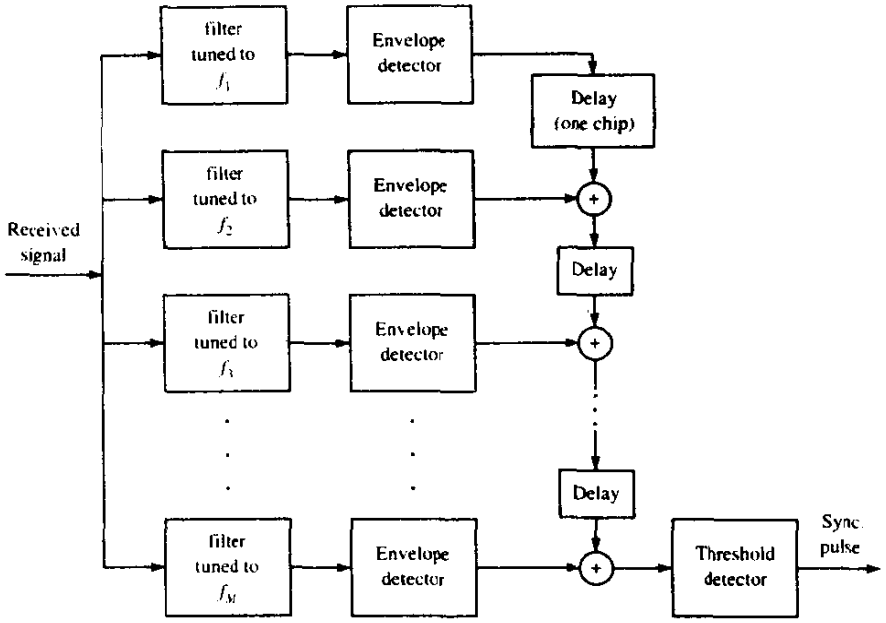

FIGURE 13-5-2 System for acquisition of a FH signal.

transmitted to the receiver. The initial acquisition system at the receiver looks for this known FH signal pattern. For example, a bank of matched filters tuned to the transmitted frequencies in the known pattern may be employed. Their outputs must be properly delayed, envelope- or square-law-detected, weighted, if necessary, and added (noncoherent integration) to produce the signal output which is compared with a threshold. A signal present is declared when the threshold is exceeded. The search process is usually performed continuously in time until a threshold is exceeded. A block diagram illustrating this signal acquisition scheme is given in Fig. 13-5-2. As an alternative, a single matched-filter–envelope detector pair may be used, preceded by a frequency-hopping pattern generator and followed by a post-detection integrator and a threshold detector. This configuration, shown in Fig. 13-5-3, is based on a serial search and is akin to the sliding correlator for DS spread spectrum signals.

The sliding correlator for the DS signals or its counterpart shown in Fig. 13-5-3 for FH signals basically perform a serial search that is generally time-consuming. As an alternative, one may introduce some degree of parallelism by having two or more such correlators operating in parallel and searching over nonoverlapping time slots. In such a case, the search time is reduced at the expense of a more complex and costly implementation. Figure 13-5-2 represents such a parallel realization for the FH signals.

During the search mode, there may be false alarms that occur at the designed false alarm rate of the system. To handle the occasional false alarms, it is necessary to have an additional method or circuit that checks to confirm

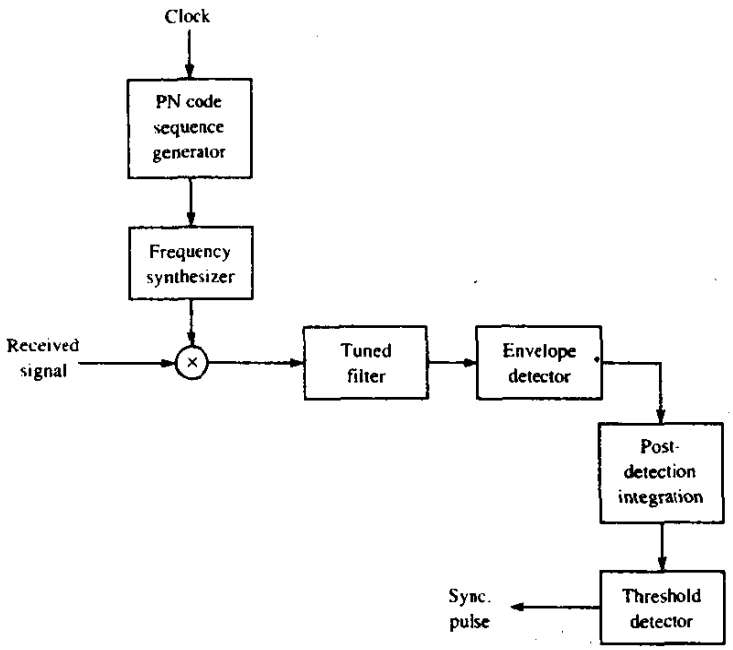

FIGURE 13-5-3 Alternative system for acquisition of a FH signal.

that the received signal at the output of the correlator remains above the threshold. With such a detection strategy, a large noise pulse that causes a false alarm will cause only a temporary exceedence of the threshold. On the other hand, when a signal is present, the correlator or matched filter output will stay above the threshold for the duration of the transmitted signal. Thus, if confirmation fails, the search is resumed.

Another initial search strategy, called a *sequential search*, has been investigated by Ward (1965, 1977). In this method, the dwell time at each delay in the search process is made variable by employing a correlator with a variable integration period whose (biased) output is compared with two thresholds. Thus, there are three possible decisions:

1 if the upper threshold is exceed by the correlator output, initial synchronization is declared established;

2 if the correlator output falls below the lower threshold, the signal is declared absent at that delay and the search process resumes at a different delay;

3 if the correlator output falls between the two thresholds, the integration time is increased by one chip and the resulting output is compared with the two thresholds again.

Hence, steps 1, 2, and 3 are repeated for each chip interval until the correlator output either exceeds the upper threshold or falls below the lower threshold.

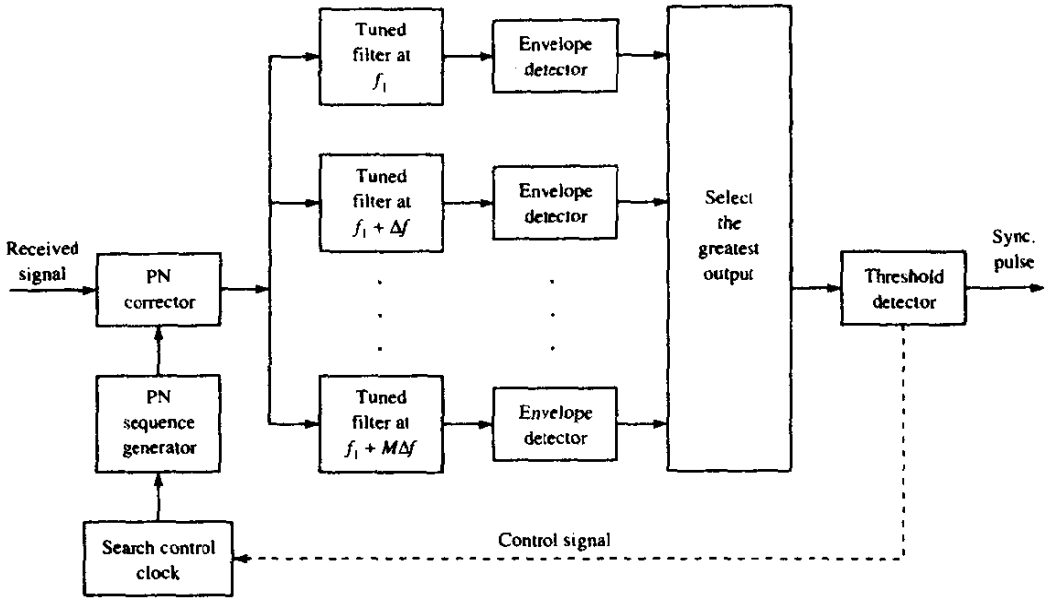

FIGURE 13-5-4 Initial search for Doppler frequency offset in a DS system.

The sequential search method falls in the class of sequential estimation methods proposed by Wald (1947), which are known to result in a more efficient search in the sense that the average search time is minimized. Hence, the search time for a sequential search is less than that for the fixed dwell time integrator.

In the above discussion, we have considered only time uncertainty in establishing initial synchronization. However, another aspect of initial synchronization is frequency uncertainty. If the transmitter and/or the receiver are mobile, the relative velocity between them results in a Doppler frequency shift in the received signal relative to the transmitted signal. Since the receiver does not usually know the relative velocity, a priori, the Doppler frequency shift is unknown and must be determined by means of a frequency search method. Such a search is usually accomplished in parallel over a suitably quantized frequency uncertainty interval and serially over the time uncertainty interval. A block diagram of this scheme is shown in Fig. 13-5-4. Appropriate Doppler frequency search methods can also be devised for FH signals.

Tracking Once the signal is acquired, the initial search process is stopped and fine synchronization and tracking begins. The tracking maintains the PN code generator at the receiver in synchronism with the incoming signal. Tracking includes both fine chip synchronization and, for coherent demodulation, carrier phase tracking.

The commonly used tracking loop for a DS spread spectrum signal is the

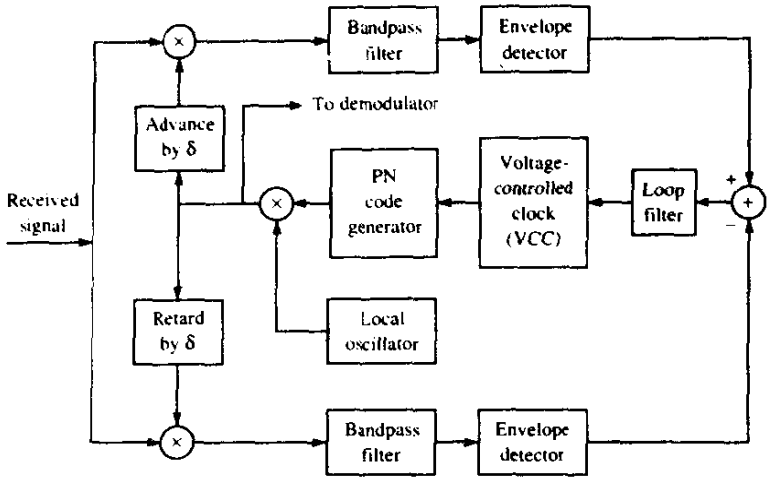

FIGURE 13-5-5 Delay-locked loop (DLL) for PN code tracking.

delay-locked loop (DLL), which is shown in Fig. 13-5-5. In this tracking loop, the received signal is applied to two multipliers, where it is multiplied by two outputs from the local PN code generator, which are delayed relative to each other by an amount $2\delta \leq T_c$. Thus, the product signals are the cross-correlations between the received signal and the PN sequence at the two values of delay. These products are bandpass-filtered and envelope- (or square-law-) detected and then subtracted. This difference signal is applied to the loop filter that drives the voltage controlled clock (VCC). The VCC serves as the clock for the PN code signal generator.

If the synchronism is not exact, the filtered output from one correlator will exceed the other and the VCC will be appropriately advanced or delayed. At the equilibrium point, the two filtered correlator outputs will be equally displaced from the peak value, and the PN code generator output will be exactly synchronized to the received signal that is fed to the demodulator. We observe that this implementation of the DLL for tracking a DS signal is equivalent to the early–late gate bit tracking synchronizer previously discussed in Section 6-3-2 and shown in Fig. 6-3-5.

An alternative method for time tracking a DS signal is to use a *tau-dither loop* (TDL), illustrated by the block diagram in Fig. 13-5-6. The TDL employs a single "arm" instead of the two "arms" shown in Fig. 13-5-5. By providing a suitable gating waveform, it is possible to make this "single-arm" implementation appear to be equivalent to the "two-arm" realization. In this case, the cross-correlation is regularly sampled at two values of delay, by stepping the code clock forward or backward in time by an amount δ. The envelope of the cross-correlation that is sampled at $\pm\delta$ has an amplitude modulation whose phase relative to the tau-dither modulator determines the sign of the tracking error.

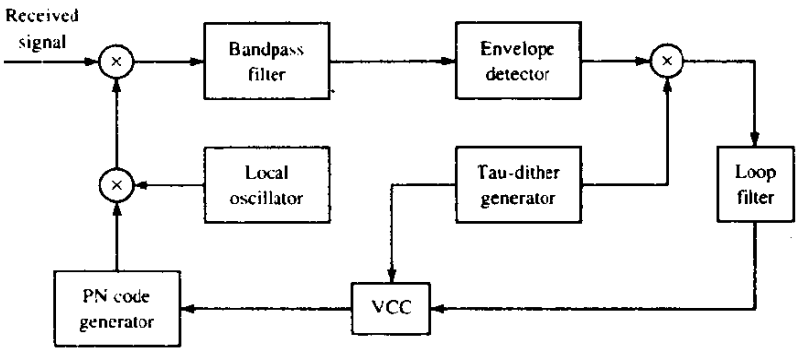

FIGURE 13-5-6 Tau-dither loop (TDL).

A major advantage of the TDL is the less costly implementation resulting from elimination of one of the two arms that are employed in the conventional DLL. A second and less apparent advantage is that the TDL does not suffer from performance degradation that is inherent in the DLL when the amplitude gain in the two arms is not properly balanced.

The DLL (and its equivalent, the TDL) generate an error signal by sampling the signal correlation function at $\pm\delta$ off the peak as shown in Fig. 13-5-7(*a*). This generates an error signal as shown in Fig. 13-5-7(*b*). The analysis of the performance of the DLL is similar to that for the phase-locked loop (PLL) carried out in Section 6-3. If it were not for the envelope detectors in the two arms of the DLL, the loop would resemble a Costas loop. In general, the variance of the time estimation error in the DLL is inversely proportional to the loop SNR, which depends on the input SNR to the loop and the loop bandwidth. Its performance is somewhat degraded as in the squaring PLL by the nonlinearities inherent in the envelope detectors, but this degradation is relatively small.

FIGURE 13-5-7 Autocorrelation function and tracking error signal for DLL.

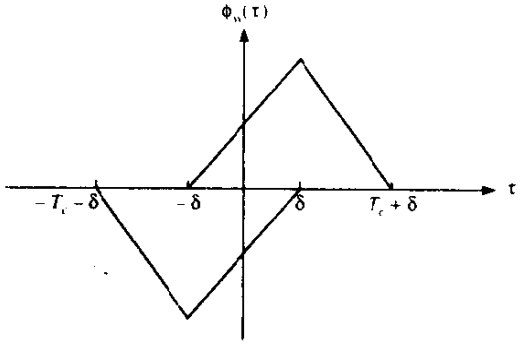

(*a*) Autocorrelation function

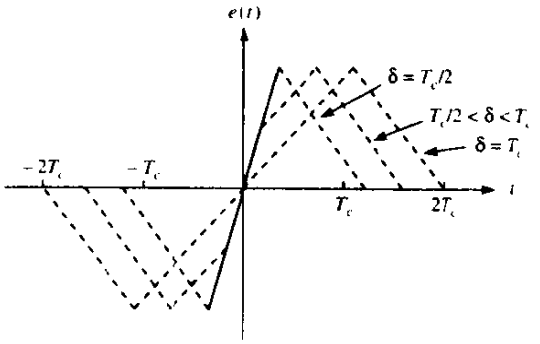

(*b*) Tracking error signal

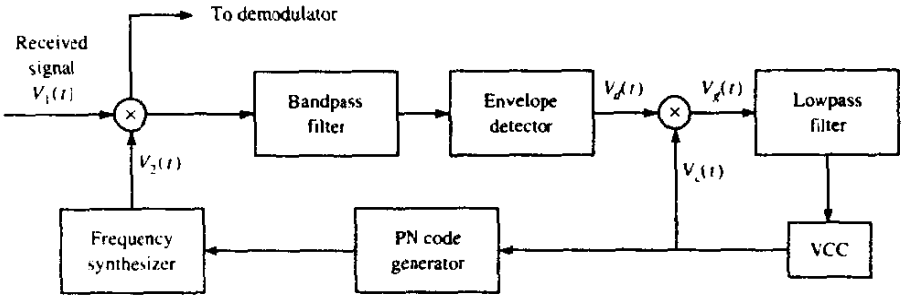

(*a*) Tracking loop for FH signals

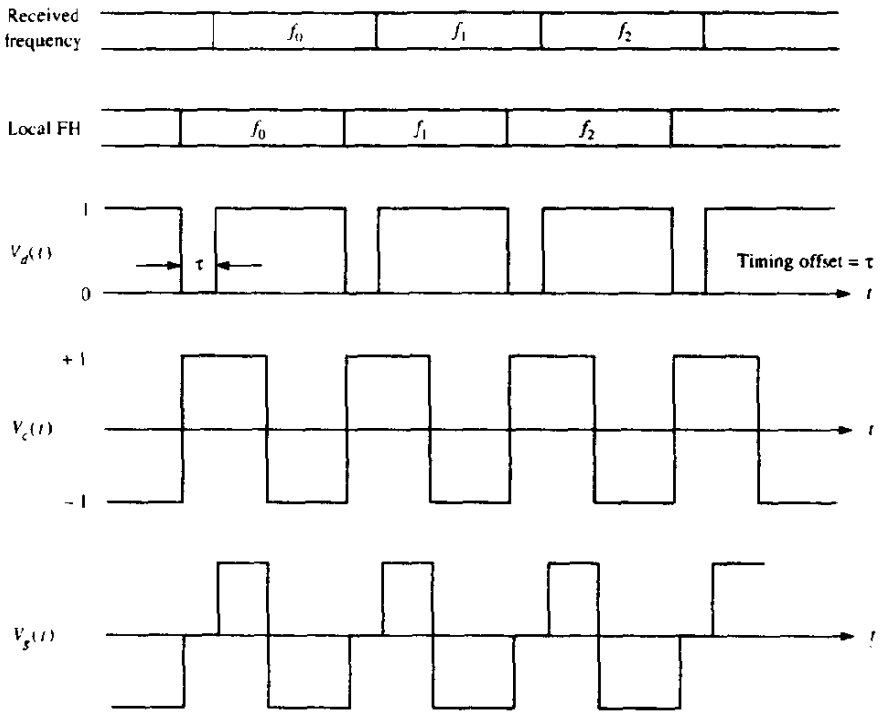

(*b*) Wavefront for tracking an FH signal

FIGURE 13-5-8 Trracking method for FH signals. [*From Pickholtz* et al. *(1982). © 1982 IEEE.*]

A typical tracking technique for FH spread spectrum signals is illustrated in Fig. 13-5-8(*a*). This method is also based on the premise that, although initial acquisition has been achieved, there is a small timing error between the received signal and the receiver clock. The bandpass filter is tuned to a single intermediate frequency and its bandwidth is of the order of $1/T_c$, where T_c is the chip interval. Its output is envelope-detected and then multiplied by the clock signal to produce a three-level signal, as shown in Fig. 13-5-8(*b*), which

drives the loop filter. Note that when the chip transitions from the locally generated sinusoidal waveform do not occur at the same time as the transitions in the incoming signal, the output of the loop filter will be either negative or positive, depending on whether the VCC is lagging or advanced relative to the timing of the input signal. This error signal from the loop filter will provide the control signal for adjusting the VCC timing signal so as to drive the frequency synthesized pulsed sinusoid to proper synchronism with the received signal.

13-6 BIBLIOGRAPHICAL NOTES AND REFERENCES

The introductory treatment of spread spectrum signals and their performance that we have given in this chapter is necessarily brief. Detailed and more specialized treatments of signal acquisition techniques, code tracking methods, and hybrid spread spectrum systems, as well as other general topics on spread spectrum signals and systems, can be found in the vast body of technical literature that now exists on the subject.

Historically, the primary application of spread spectrum communications has been in the development of secure (AJ) digital communication systems for military use. In fact, prior to 1970, most of the work on the design and development of spread spectrum communications was classified. Since then, this trend has been reversed. The open literature now contains numerous publications on all aspects of spread spectrum signal analysis and design. Moreover, we have recently seen publications dealing with the application of spread spectrum signaling techniques to commercial communications such as interoffice radio communications (see Pahlavan, 1985) and mobile-user radio communications (see Yue, 1983).

A historical perspective on the development of spread spectrum communication systems covering the period 1920–1960 is given in a paper by Scholtz (1982). Tutorial treatments focusing on the basic concepts are found in the papers by Scholtz (1977) and Pickholtz *et al.* (1982). These papers also contain a large number of references to previous work. In addition, there are two papers by Viterbi (1979, 1985) that provide a basic review of the performance characteristics of DS and FH signaling techniques.

Comprehensive treatments of various aspects of analysis and design of spread spectrum signals and systems, including synchronization techniques are now available in the texts by Simon *et al.* (1985), Ziemer and Peterson (1985), and Holmes (1982). In addition to these texts, there are several special issues of the *IEEE Transactions on Communications* devoted to spread spectrum communications (August 1977 and May 1982) and the *IEEE Transactions on Selected Areas in Communication* (September 1985, May 1989, May 1990, and June 1993). These issues contain a collection of papers devoted to a variety of topics, including multiple access techniques, synchronization techniques, and performance analyses with various types of interference. A number of important papers that have been published in IEEE journals have also been reprinted in book form by the IEEE Press (Dixon, 1976; Cook *et al.* 1983).

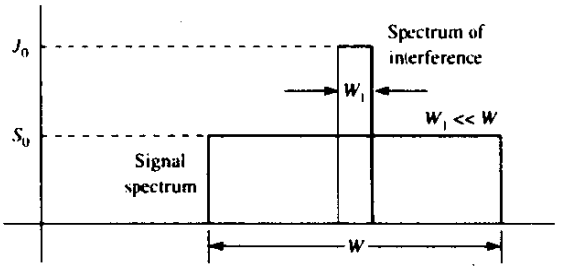

FIGURE P13-2

Finally, we recommend the book by Golomb (1967) as a basic reference on shift register sequences for the reader who wishes to delve deeper into this topic.

PROBLEMS

13-1 Following the procedure outlined in Example 13-2-2, determine the error rate performance of a DS spread spectrum system in the presence of CW jamming when the signal pulse is

$$g(t) = \sqrt{\frac{16\mathscr{E}_c}{3T_c}} \cos^2\left[\frac{\pi}{T_c}(t - \tfrac{1}{2}T_c)\right], \quad 0 \le t \le T_c$$

13-2 The sketch in Fig. P13-2 illustrates the power spectral densities of a PN spread spectrum signal and narrowband interference in an uncoded (trivial repetition code) digital communication system. Referring to Fig. 13-2-6, which shows the demodulator for this signal, sketch the (approximate) spectral characteristics of the signal and the interference after the multiplication of $r(t)$ with the output of the PN generator. Determine the fraction of the total interference that appears at the output of the correlator when the number of PN chips per bit is L_c.

13-3 Consider the concatenation of a Reed–Solomon (31, 3) ($q = 32$-ary alphabet) as the outer code with a Hadamard (16, 5) binary code as the inner code in a DS spread spectrum system. Assume that soft-decision decoding is performed on both codes. Determine an upper (union) bound on the probability of a bit error based on the minimum distance of the concatenated code.

13-4 The Hadamard $(n, k) = (2^m, m + 1)$ codes are low-rate codes with $d_{\min} = 2^{m-1}$. Determine the performance of this class of codes for DS spread spectrum signals with binary PSK modulation and either soft-decision or hard-decision decoding.

13-5 A rate 1/2 convolutional code with $d_{\text{free}} = 10$ is used to encode a data sequence occurring at a rate of 1000 bits/s. The modulation is binary PSK. The DS spread-spectrum sequence has a chip rate of 10 MHz.

a Determine the coding gain.

b Determine the processing gain.

c Determine the jamming margin assuming an $\mathscr{E}_b/J_0 = 10$.

13-6 A total of 30 equal-power users are to share a common communication channel by CDMA. Each user transmits information at a rate of 10 kbits/s via DS spread-spectrum and binary PSK. Determine the minimum chip rate to obtain a bit error

probability of 10^{-5}. Additive noise at the receiver may be ignored in this computation.

13-7 A CDMA system is designed based on DS spread spectrum with a processing gain of 1000 and binary PSK modulation. Determine the number of users if each user has equal power and the desired level of performance is an error probability of 10^{-6}. Repeat the computation if the processing gain is changed to 500.

13-8 A DS spread-spectrum system transmits at a rate of 1000 bits/s in the presence of a tone jammer. The jammer power is 20 dB greater than the desired signal and the required $\mathscr{E}_b/J_0$ to achieve satisfactory performance is 10 dB.

a Determine the spreading bandwidth required to meet the specifications.

b If the jammer is a pulse jammer, determine the pulse duty cycle that results in worst-case jamming and the corresponding probability of error.

13-9 A CDMA system consists of 15 equal-power users that transmit information at a rate of 10 000 bits/s, each using a DS spread spectrum signal operating at a chip rate of 1 MHz. The modulation is binary PSK.

a Determine the $\mathscr{E}_b/J_0$, where J_0 is the spectral density of the combined interference.

b What is the processing gain?

c How much should the processing gain be increased to allow for doubling the number of users without affecting the output SNR?

13-10 A DS binary PSK spread spectrum signal has a processing gain of 500. What is the jamming margin against a continuous-tone jammer if the desired error probability is 10^{-5}?

13-11 Repeat Problem 13-10 if the jammer is a pulsed-noise jammer with a duty cycle of 1%.

13-12 Consider the DS spread spectrum signal

$$c(t) = \sum_{n=-\infty}^{\infty} c_n p(t - nT_c)$$

where c_n is a periodic m sequence with a period $N = 127$ and $p(t)$ is a rectangular pulse of duration $T_c = 1\ \mu$s. Determine the power spectral density of the signal $c(t)$.

13-13 Suppose that $\{c_{1i}\}$ and $\{c_{2i}\}$ are two binary (0, 1) periodic sequences with periods N_1 and N_2, respectively. Determine the period of the sequence obtained by forming the modulo-2 sum of $\{c_{1i}\}$ and $\{c_{2i}\}$.

13-14 An $m = 10$ ML shift register is used to generate the pseudorandom sequence in a DS spread spectrum system. The chip duration is $T_c = 1\ \mu$s, and the bit duration is $T_b = NT_c$, where N is the length (period) of the m sequence.

a Determine the processing gain of the system in dB.

b Determine the jamming margin if the required $\mathscr{E}_b/J_0 = 10$ and the jammer is a tone jammer with an average power J_{av}.

13-15 A FH binary orthogonal FSK system employs an $m = 15$ stage linear feedback shift register that generates an ML sequence. Each state of the shift register selects one of L nonoverlapping frequency bands in the hopping pattern. The bit rate is 100 bits/s and the hop rate is once per bit. The demodulator employs noncoherent detection.

a Determine the hopping bandwidth for this channel.

b What is the processing gain?

c What is the probability of error in the presence of AWGN?

13-16 Consider the FH binary orthogonal FSK system described in Problem 13-15. Suppose that the hop rate is increased to 2 hops/bit. The receiver uses square-law combining to combine the signal over the two hops.
- **a** Determine the hopping bandwidth for the channel.
- **b** What is the processing gain?
- **c** What is the error probability in the presence of AWGN?

13-17 In a fast FH spread-spectrum system, the information is transmitted via FSK, with noncoherent detection. Suppose there are $N = 3$ hops/bit, with hard-decision decoding of the signal in each hop.
- **a** Determine the probability of error for this system in an AWGN channel with power spectral density $\frac{1}{2}N_0$ and an SNR = 13 dB (total SNR over the three hops).
- **b** Compare the result in (a) with the error probability of a FH spread-spectrum system that hops once per bit.

13-18 A slow FH binary FSK system with noncoherent detection operates at $\mathscr{E}_b/J_0 = 10$, with a hopping bandwidth of 2 GHz, and a bit rate of 10 kbits/s.
- **a** What is the processing gain for the system?
- **b** If the jammer operates as a partial-band jammer, what is the bandwidth occupancy for worst-case jamming?
- **c** What is the probability of error for the worst-case partial-band jammer?

13-19 Determine the error probability for a FH spread spectrum signal in which a binary convolutional code is used in combination with binary FSK. The interference on the channel is AWGN. The FSK demodulator outputs are square-law detected and passed to the decoder, which performs optimum soft-decision Viterbi decoding as described in Section 8-2. Assume that the hopping rate is 1 hop per coded bit.

13-20 Repeat Problem 13-19 for hard-decision Viterbi decoding.

13-21 Repeat Problem 13-19 when fast frequency hopping is performed at a hopping rate of L hops per coded bit.

13-22 Repeat Problem 13-19 when fast frequency hopping is performed with L hops per coded bit and the decoder is a hard-decision Viterbi decoder. The L chips per coded bit are square-law-detected and combined prior to the hard decision.

13-23 The TATS signal described in Section 13-3-3 is demodulated by a parallel bank of eight matched filters (octal FSK), and each filter output is square-law-detected. The eight outputs obtained in each of seven signal intervals (56 total outputs) are used to form the 64 possible decision variables corresponding to the Reed-Solomon (7, 2) code. Determine an upper (union) bound of the code word error probability for AWGN and soft-decision decoding.

13-24 Repeat Problem 13-23 for the worst-case partial-band interference channel.

13-25 Derive the results in (13-2-62) and (13-2-63) from (13-2-61).

13-26 Show that (13-3-14) follows from (13-3-13).

13-27 Derive (13-3-17) from (13-3-16).

13-28 The generator polynomials for constructing Gold code sequences of length $n = 7$ are

$$g_1(p) = p^3 + p + 1$$
$$g_2(p) = p^3 + p^2 + 1$$

Generate all the Gold codes of length 7 and determine the cross-correlations of one sequence with each of the others.

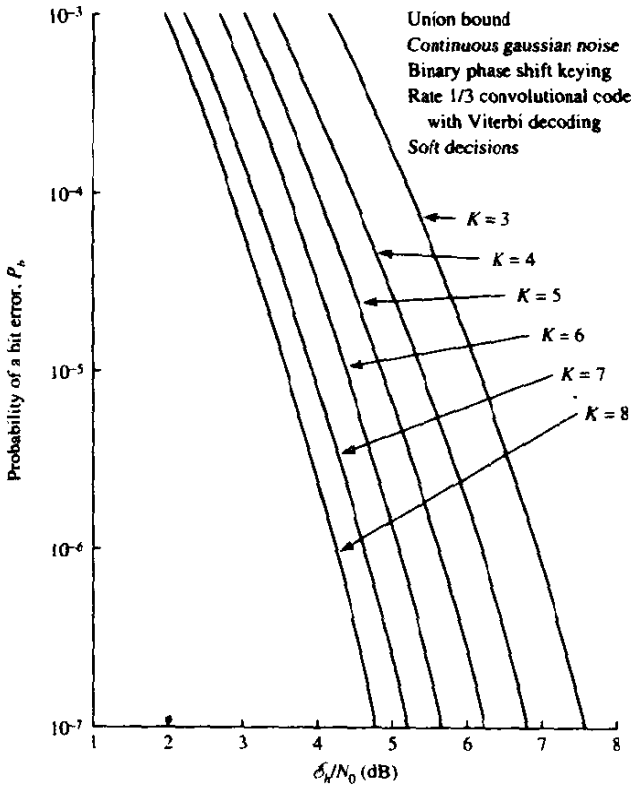

FIGURE P13-29

13-29 In Section 13-2-3, we demonstrated techniques for evaluating the error probability of a coded system with interleaving in pulse interference by using the cutoff rate parameter R_0. Use the error probability curves given in Fig. P13-29 for rate 1/2 and 1/3 convolutional codes with soft-decision Viterbi decoding to determine the corresponding error rates for a coded system in pulse interference. Perform this computation for $K = 3$, 5, and 7.

13-30 In coded and interleaved DS binary PSK modulation with pulse jamming and soft-decision decoding, the cutoff rate is

$$R_0 = 1 - \log_2 (1 + \alpha e^{-\alpha \mathscr{E}_c/N_0})$$

where α is the fraction of the time the system is being jammed, $\mathscr{E}_c = \mathscr{E}_b R$, R is the bit rate, and $N_0 \equiv J_0$.

a Show that the SNR per bit, $\mathscr{E}_b/N_0$, can be expressed as

$$\frac{\mathscr{E}_b}{N_0} = \frac{1}{\alpha R} \ln \frac{\alpha}{2^{1-R_0} - 1}$$

b Determine the value of α that maximizes the required $\mathscr{E}_b/N_0$ (worst-case pulse jamming) and the resulting maximum value of $\mathscr{E}_b/N_0$.

b Plot the graph of $10 \log (\mathscr{E}_b/rN_0)$ versus R_0, where $r = R_0/R$, for worst-case pulse jamming and for AWGN ($\alpha = 1$). What conclusions do you reach regarding the effect of worst-case pulse jamming?

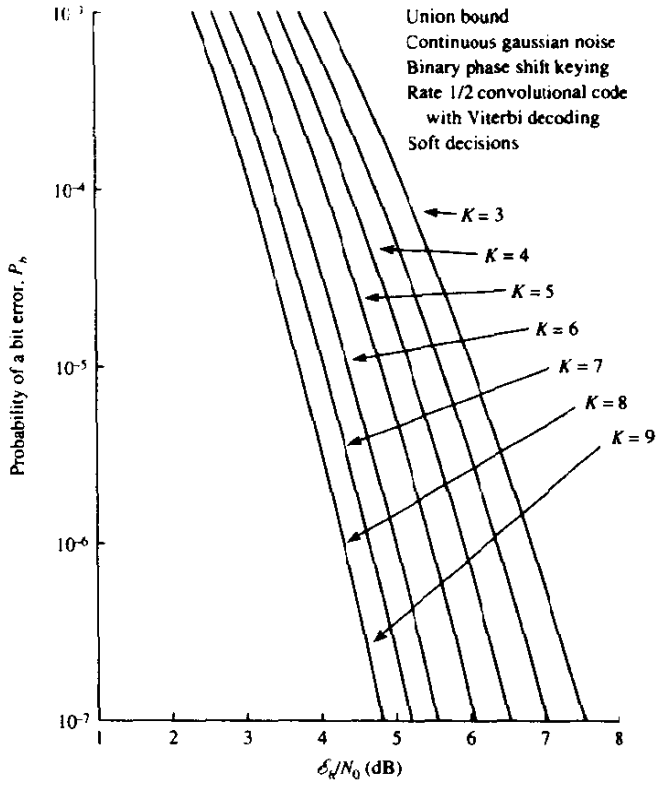

FIGURE P13-29 *(Continued).*

13-31 In a coded and interleaved frequency-hopped q-ary FSK modulation with partial band jamming and coherent demodulation with soft-decision decoding, the cutoff rate is

$$R_0 = \log_2 \left[\frac{q}{1 + (q-1)\alpha e^{-\alpha \mathscr{E}_c/2N_0}} \right]$$

where α is the fraction of the band being jammed, $\mathscr{E}_c$ is the chip (or tone) energy, and $N_0 = J_0$.

a Show that the SNR per bit can be expressed as

$$\frac{\mathscr{E}_b}{N_0} = \frac{2}{\alpha R} \ln \frac{(q-1)\alpha}{q2^{-R_0} - 1}$$

b Determine the value of α that maximizes the required $\mathscr{E}_b/N_0$ (worst-case partial band jamming) and the resulting maximum value of $\mathscr{E}_b/N_0$.

c Define $r = R_0/R$ in the result for $\mathscr{E}_b/N_0$ from (b), and plot $10 \log (\mathscr{E}_b/rN_0)$ versus the normalized cutoff rate $R_0/\log_2 q$ for $q = 2, 4, 8, 16, 32$. Compare these graphs with the results of Problem 13-30(c). What conclusions do you reach regarding the effect of worst-case partial band jamming? What is the effect of increasing the alphabet size q? What is the penalty in SNR between the results in Problem 13-30(c) and q-ary FSK as $q \to \infty$?